Tectonic control on Jurassic to Early Cretaceous sedimentation in the Dutch Central Graben; an integrated analysis of seismic and well log data

Gijsbert Anne van Dijk, March 2021, ***final version***

First advisor: Prof. dr. Liviu Matenco

Second advisor: Prof. dr. Fadi Nader

Abstract

One of the best illustrations of the complex interplay between extensional faulting, salt movement and eustasy is the deposition of the Jurassic to Early Cretaceous sediments in the Dutch Central Graben. We have quantified this deposition by a multi-scale tectonic successions approach employing two ENE-WSW seismic sections perpendicular to the strike of the basin. Our structural reconstruction of the interpreted seismic sections can be grouped in three main phases of basin development, starting with initial deposition focused on the basin center during sedimentation of the Schieland Group. This initial period was followed by deposition along the former basin margins in rim-synclines, which was coeval with the formation of well-documented turtle anticlines during sedimentation of the Scruff Group, followed by tectonic inversion. Building over the well-studied stratigraphic framework in the Dutch offshore, we present a higher resolution well-logs and seismic model of the Jurassic - Early Cretaceous which is able to differentiate 6 to 8 tectonic successions during the deposition of the Schieland Group. These tectonic successions demonstrate a laterally variable alternation of tectonic activity and quiescence controlling sedimentation. This interpretation contrasts with the analysis of the marginal Scruff Group, where results show that 3rd order sea-level fluctuations are the major control on observed sedimentary cyclicity expressed in well log and lithological data. Furthermore, the lateral variability of tectonic successions between the studied transects highlights the importance of local variability in deposition and facies distribution during syn-rift sedimentation in space and over time.

Table of Contents

1. Introduction

Tectonics, eustasy, and climate exert major controls on the evolution of the stratigraphic record of sedimentary basins. The formation of the Dutch Central Graben and surrounding areas results from the complex interplay between these controlling factors. The Jurassic to Cretaceous basin infill of the Dutch Central Graben is characterized by an alternation of marine and continental facies and high diachroneity of lithological formations, deposited in a rapidly subsiding, relatively narrow salt-influenced rift basin.

The current stratigraphic framework offshore Netherlands results from the accumulation of a large amount of data (Abbink et al., 2006; Herngreen et al., 2003; Van Adrichem Boogaert and Kouwe, 1993). Recent studies describe the occurrence and distribution of three Tectonic Megasequences by the means of interpreting seismic and well data (Bouroullec et al., 2018; Verreussel et al., 2018). This approach provides a robust framework for Jurassic - Cretaceous strata in the Dutch Central Graben, but potentially neglects local variability in development of the basin. First of all, extension is assumed to be coevally active over the entire area, while extensional basins are dynamic systems and laterally variable in their evolution. Secondly, other mechanisms that control accommodation space creation, such as eustasy, climate, and in particular highly variable salt re-distribution in space and over time, are less well considered and not separated in their relative contributions. Furthermore, the Dutch Central Graben, like any other extensional system, is characterized by multi-order depositional cyclicity, which is less addressed or understood by present studies.

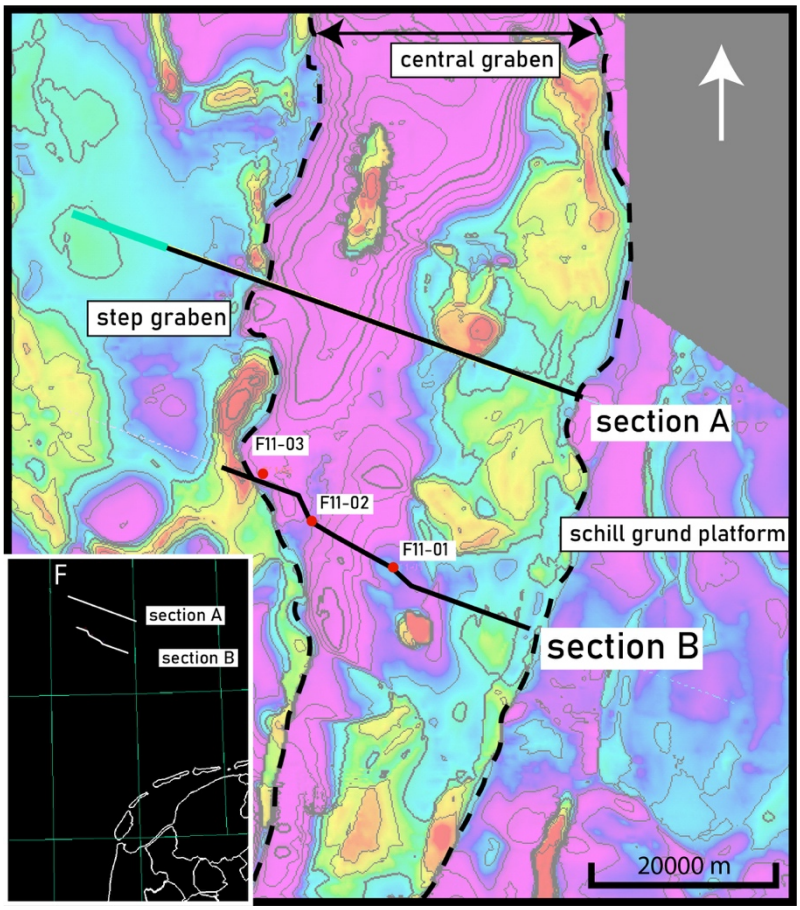

Figure 1. Base of map of the study area. Colours indicate the top of the Jurassic Altena Group, delineating the Dutch Central Graben. Section A and B are indicated. Both cross-sections are roughly perpendicular to the axis of the Dutch Central Graben. Section B is a composite section of 2D seismic and 3D seismic data.

State of the art tectono-sedimentary studies of tectonically active sedimentary systems require a multi- observational framework (outcrops, cores, seismic and/or well log data) able to derive the key controlling parameters (Catuneanu, 2019a, 2019b; Matenco and Haq, 2020). This approach should be, ideally, largely independent of causal mechanisms, in order to be applicable to a wide variety of settings and controlling mechanisms (Neal et al., 2016). Classic sequence stratigraphy was developed for stable passive margin settings where long term thermal subsidence and superposed orders of eustatic movements control the basin infill (Mitchum et al., 1977; Wagoner et al., 1990). The sequence stratigraphic nomenclature was

subsequently applied to various other sedimentary basins where underlying allogenic forcing mechanisms differ significantly. This is true in particular for active tectonic basins, such as the Jurassic-Cretaceous evolution of the Dutch Central Graben, where the standard sequence stratigraphic nomenclature is rather difficult to be applied due to reasons such as unclear shoreline reference levels, fault-induced re-distribution of sediments or endemic restrictions. Therefore, a different tectono-sedimentary, observation-based approach is required in such basins. Among various alternatives available, (Matenco and Haq, 2020) proposed a conceptual model that defines tectonic successions bounded by sequence boundaries comprising sourceward and basinward migrating facies tracts that are governed by the relative roles of accommodation space creation and sediment supply. Facies tracts are defined by the integration of seismic data (stratal stacking patterns and seismic facies), well logs (grain size trends, well log facies), and lithological data (core or side wall samples). In this model, sea-level variations may have a subordinate influence on sediment deposition in the early stages of rift basin formation.

In our research, we aim to understand the allogenic and autogenic forcing factors controlling the Jurassic-Cretaceous evolution of the Dutch Central Graben by the means of a high-resolution study of available seismic, well-logs and core data. We build from the tectonostratigraphic framework previously defined (Abbink et al., 2006; Verreussel et al., 2018) by accounting for the spatio-temporal variability of deposition and its controlling factors. We have interpreted a number of ENE-WSW oriented key transects (Figure 1) crossing the Dutch Central Graben that link the flanks of the main salt diapirs and cross a number of important correlation wells. We start with seismic interpretation and restoration followed by a higher resolution analysis of public well logs (F11-01, F11-02, F11-03), cores and well-report data (available at nlog.nl and dinoloket.nl), including information on biostratigraphy, lithology and palynology. The analysed dataset is used to define tectonic successions controlled by variable types of allogenic or autogenic forcing factors. The results demonstrate that tectonic successions provide a much higher-resolution tectono-stratigraphic framework when compared with previously defined tectonic mega-sequences. This improves the definition of spatio-temporal variability and the discrimination between salt-, tectonic- and eustatic-driven forcing.

2. Geological framework

2.1 Tectonic Evolution

The Dutch Central Graben is one of the main structural elements of the Dutch offshore, a key part of the general North Sea Central Graben. It is an elongated, NNW-SSE to N-S trending salt-bounded basin, bordered by the Step Graben (SG) to the west, and the Schill Grund Platform (SGP) to the east (figure 2). To the southeast, it borders the Terschelling Basin (TB) and Vlieland basin (VB). The Permian to Cenozoic evolution of the Dutch Central Graben and surrounding structural elements can be subdivided into three general periods.

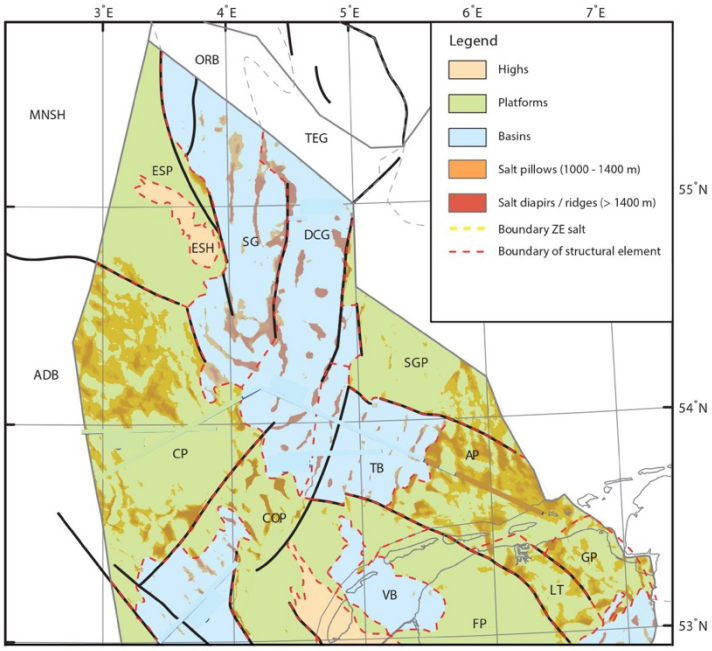

Figure 2. Structural elements of the Dutch Central Graben and surrounding areas (modified from ten Veen, 2012). ORB = Outer Rough Basin, TEG = Tail End Graben, MNSH = Mid-North Sea High, ESP = Elbow Spit Platform , SG = Step Graben, DCG = Dutch Central Graben, ESH = Elbow Spit High, SGP = Schill Grund Platform, ADB = Anglo-Dutch Basin, CP = Cleaverbank Platform, COP = Central Offshore Platform, TB = Terschelling Basin, AP = Ameland Platform, VB = Vlieland Basin, FP = Friesland Platform, GP = Groningen Platform, LT = Lauwerszee Trough.

2.1.1 Permo-Triassic

The Permo-Triassic basins in the Dutch northern offshore are the successors of a large foredeep that was located north of the Variscan orogen (Van Wijhe, 1987). These basins are part of the larger Southern Permian Basin, typically described as a 'passive' subsidence, sag-type basin. In the aftermath of Variscan continental collision, wrench tectonics and magmatism became widespread in north-western Europe, resulting in significant thinning and thermal destabilization of the lithosphere (van Wees et al., 2000). The deposition of extensive Early Permian volcanic deposits attests to the dominant tectono-magmatic control of this period. Passive thermal subsidence following thermal destabilization accounts for most of the Permian and Triassic subsidence, as inferred from quantitative subsidence analyses and forward basin modelling (van Wees et al., 2000). This subsidence accommodated widespread sedimentation of Rotliegend clastic deposits (Geluk, 2005). Continued subsidence, together with the establishment of marine connectivity with the Arctic Ocean resulted in cyclic periods of thick Zechstein halite sequences, intercalated with carbonates during the Late Permian (Geluk, 2005; Van Wijhe, 1987). This cyclic deposition, interpreted to be glacio-eustatic driven, resulted in the deposition of five distinct evaporite members, overlying Rotliegend clastics and thinning in a southward direction. The maximum southern extent can be locally placed at the northern onshore NL limit (ten Veen et al., 2012).

The rifting between Greenland and Scandinavia that commenced during Triassic times eventually created an eastern branch that propagated southwards into the North Sea area, coeval with a gradual decrease of tectonic activity over time (Pharaoh et al., 2010). Thickness and distribution of Early Triassic Buntsandstein clastics and overlying Muschelkalk carbonates indicate persistence of thermal subsidence into Triassic times in the Dutch Central Graben area (Geluk, 2005). Seismic data indicates some thickness variations of Triassic strata across faults

(Wong et al., 2007), evidencing an increasing role of crustal extension in the creation of accommodation space. Rifting accelerated during the Early-Kimmerian in the Late Triassic, while development of salt walls during Middle Triassic times indicate the first stages of active diapirism triggered by rift-related faulting (Remmelts, 1996, 1995). Due to the difficulty of sub-salt seismic imaging and due to Mesozoic remobilization of Zechstein evaporites, a good interpretation of sub-salt geometries and connection with the overlying Triassic syn-kinematic sedimentation is difficult (Pharaoh et al., 2010), thereby complicating direct qualitative and quantitative interpretations of crustal extension in the Permian or Triassic.

2.1.2 Jurassic

The Early Jurassic saw a continuation of the low tectonic activity that characterized most of the Permo-Triassic basin evolution. Uniform and regional thermal subsidence combined with a general eustatic sea-level rise (Haq et al., 1988) and local (but relatively minor) fault-controlled subsidence caused widespread deposition of an open marine facies in the form of the Early Jurassic Altena Group (Pharaoh et al., 2010; Wong et al., 2007). Anoxic conditions, resulting from stagnant water phases within this basin resulted in the deposition of the thick characteristic shales of the Posidonia Shale Formation (Trabucho-Alexandre et al., 2012).

The Middle Jurassic (Toarcian to Aalenian) is characterized by a period of erosion and/or non-deposition expressed by the occurrence of a Mid-Kimmerian unconformity over large parts of the North Sea area. This unconformity truncates earlier Jurassic and Triassic strata and is mostly attributed to a phase of uplift in the central North Sea area in response to the emplacement of a mantle plume (Underhill and Partington, 1993). However, a recent study has suggested that the Aalenian regression, commonly linked to the Mid-Cimmerian Unconformity is recorded on a wider extent (Paris Basin, Tethyan Arabian Margin), and that the combination of a major Aalenian sea-level fall and the low amount of initial accommodation space (due to rift shoulder denudation) does not require a thermal dome to explain the Mid-Cimmerian Unconformity (Lafosse, 2018, internal confidential report).

The structural elements that are most evident in the present subsurface started forming during Late Jurassic times. Upper Jurassic strata are often eroded and almost exclusively preserved within the margins of the Dutch Central Graben, bordered by large salt structures. Outside this deposition, Upper Jurassic strata are solely found in either rim synclines bordering salt structures, or transverse fault zones. Locally, thin layers of Jurassic sediments have likely accumulated more uniformly over platform areas, but were later eroded. Accommodation space was created rapidly and depocenters shifted frequently, mostly controlled by sub-salt faulting and (re-)mobilization of Permian (and to a lesser extent Triassic) evaporites (Bouroullec et al., 2018; Winden et al., 2018). Uplift and erosion took place over local highs, such as the Cleaver Bank High (Cleaverbank Platform, figure 2) and Broad Fourteens High, which likely acted as a source area for clastics sediments to the South (Pharaoh et al., 2010). The Upper Jurassic sediments are highly variable in their lithofacies and depositional environment in the entire Central Graben (Dutch and Danish) system (Verreussel et al., 2018). The interfingering and high degree of diachroneity of Jurassic lithological formations and their boundaries complicates accurate correlation. Based on facies analysis of lithostratigraphic formations, it is assumed that the basin deepened southwards.

2.1.4 Cretaceous and Cenozoic

The rifting continued and generally decreased during Early Cretaceous times, associated with a general change to more distal facies deposition. The continental deposition of the Schieland Group was replaced by deposition of the marine Scruff and Rijnland groups. Both subsidence

as well as eustatic sea-level rise accommodated an overall transgression (Haq et al., 1988; Munsterman et al., 2012). By Albian times, the crustal extension had ceased in the North Sea region (Pharaoh et al., 2010). The continued sea-level rise and thermal subsidence resulted in deposition of the up to 2 km thick Chalk group, which thins towards basin axes due erosion created by subsequent inversion. Plate reorganizations associated with the Alpine Orogeny affected the entire area of the North Sea by a build-up of compressional stress, culminating in several inversion phases. The first (Sub-Hercynian) occurred in the Campanian, followed by a second (the Laramide) occurring at the start of the Cenozoic. In the Dutch Central Graben inversion is mostly observed by the upwarping of Mesozoic basin fills in broad anticlines and truncation of these basin fills along the axes of these anticlines (Van Wijhe, 1987). These axes coincide with the Jurassic to Early Cretaceous basin depocenters. The presence of salt decoupled the deformation in such a way that the overlying structures are often not directly connected with the ones observed in the underlying basement.

2.2 Lithostratigraphy

2.2.1 Stratigraphic subdivision of the Late Jurassic and Early Cretaceous

Several frameworks have been proposed to subdivide Jurassic and Cretaceous strata in the Dutch Central Graben into distinct lithostratigraphic, tectonostratigraphic or sequence stratigraphic sequences. The first stratigraphic framework for the Jurassic of the Dutch offshore was proposed by NAM and RGD in the 1980s' and was revised by van Adrichem, Boogaert and Kouwe (1993), who started to apply sequence stratigraphic concepts to the Jurassic-Cretaceous basin infills in the Dutch offshore. Herngreen (2003) tied regressive transgressive events to the sea-level cycle fluctuations published by Haq (1988). A threefold subdivision was

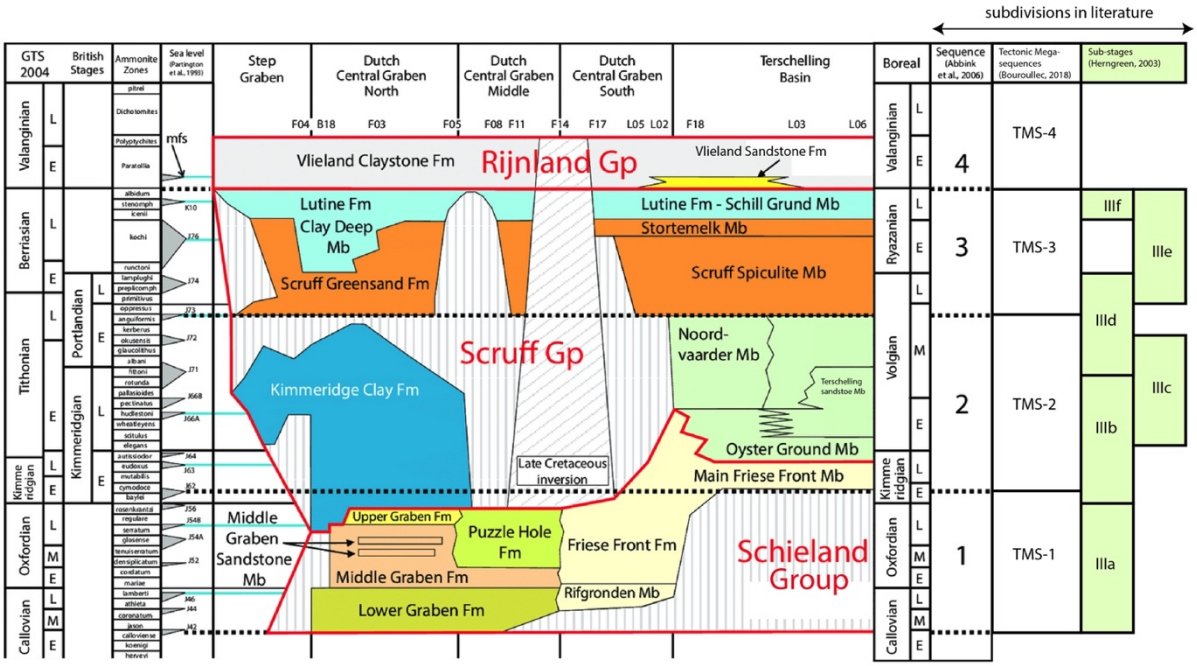

Figure 3. Stratigraphic Framework for the Jurassic-Lower Cretaceous of the Dutch offshore. On the right side of the diagram, the subdivisions that are discussed in the text are indicated. This figure is an adjusted version of a figure by Munsterman (2011). Subdivisions are based on several publications (Bouroullec et al., 2018; Verreussel et al., 2018; Abbink et al., 2006; Herngreen et al., 2003). The entire succession corresponds roughly to Megasequence 3 as defined by Herngreen (2003).

subsequently proposed by Abbink (2006), later revised and updated by Munsterman (2011) (figure 3). Herngreen (2003) subdivided the entire Dutch Jurassic into three mega-sequences, covering not only the Dutch Central Graben but also the Lower Saxony Basin and the NW-SE

trending system of basins in the onshore and western offshore (West and Central Netherlands Basin, Broad Fourteens Basin and Roer Valley Graben), while subdividing Megasequence 3 into 6 substages. These 6 substages cover the same period as the threefold subdivision of Callovian – Ryazanian strata made by Abbink (2006) and later revised and updated by Munsterman (2011). The more recent study of Bouroullec (2018) used the threefold subdivision by Abbink (2006) for a focused analysis of the Dutch Central Graben tectono-stratigraphy by defining similar tectonic mega-sequences by the means of seismic and well data analysis.

Lower and Middle Jurassic (Megasequence 1 and Megasequence 2)
Megasequence 1 as defined by Herngreen (2003) represent the continuous marine deposits of the Lower Jurassic Altena Group. This unit was named a pre-rift to early syn-rift unit by Wong (2007). Megasequence 2 is characterized by non-deposition in the Dutch central Graben and uplift and erosion of Lower Jurassic and Triassic strata at the basin margins.

Upper Jurassic to Lower Cretaceous (Megasequence 3)
Megasequence 3 (Herngreen, 2003) is structurally more complex. Wong (2007) defines this largely continental sequence as a syn-rift unit, characterized by significant lateral variation in lithologies. The first stage of this Megasequence spans the Middle Callovian and Oxfordian, referred to as stage 3a (Herngreen, 2003), Sequence 1 (Abbink, 2006), or TMS-1 (Bouroullec, 2018). Sedimentation resumed in the Dutch Central Graben after a period of non-deposition. The lowermost lithological unit, the **Lower Graben Formation**, consists of greyish-brown well-sorted sandstones that occur in 10 m thick beds, interbedded with siltstones and claystones. Some distinct coal layers are recognized, but not to a similar degree as the younger

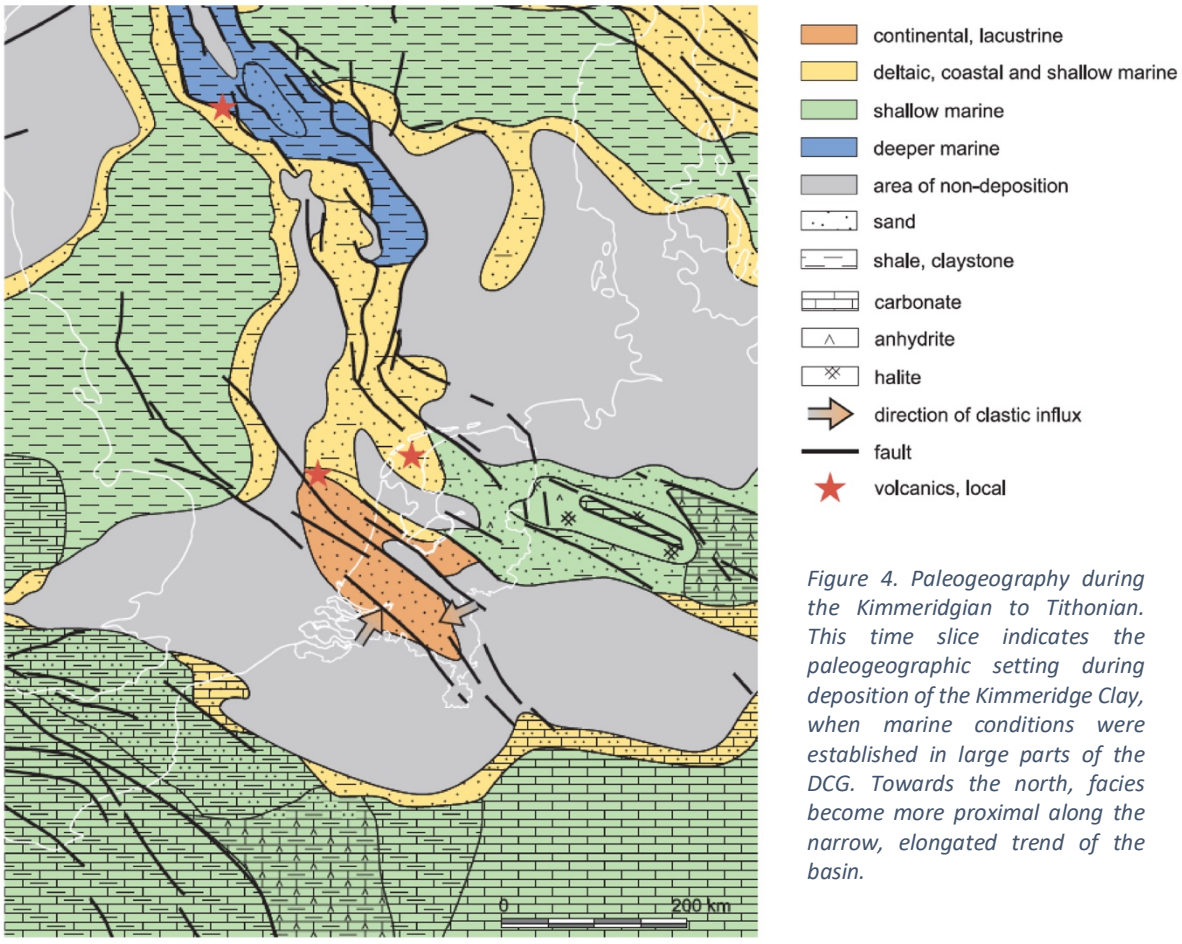

Figure 4. Paleogeography during the Kimmeridgian to Tithonian. This time slice indicates the paleogeographic setting during deposition of the Kimmeridge Clay, when marine conditions were established in large parts of the DCG. Towards the north, facies become more proximal along the narrow, elongated trend of the basin.

continental units in the Schieland Group (Munsterman, 2011). Generally, the basal part of the Lower Graben Formation is interpreted as non-marine fluvial, overlain by more marine facies towards the top, which are sand-rich and influenced by tides (Bouroullec, 2018).

The overlying **Middle Graben Formation** extends further in depositional area and is more fine-grained in character. It contains a section of grey, silty, carbonaceous claystones, intercalated locally with a sandstone member (Middle Graben Sandstone Member). Three very distinctive coal layers occur at the base of the succession. Its depositional setting is interpreted to be a lacustrine to marginal marine embayment, with poor connection to the sea. Marine palynomorphs are encountered locally, attesting to periodic sea influxes.

The deposits that overly the Middle Graben Formation are subdivided into three lithological formations, of which the southernmost Friese Front Formation represents the most proximal facies, connecting laterally to the Puzzle Hole Formation and Upper Graben Formation, and locally to the oldest part of the Kimmeridge Clay Formation. The wells in the studied F11 area penetrate the **Puzzle Hole Formation,** which was previously considered to be a sandy interval within the Kimmeridge Clay Formation (Scruff Group), but was later reassigned to the Schieland Group based on its terrestrial-paralic character (Munsterman et al., 2012). The Puzzle Hole Formation is characterized by an alternation of carbonaceous claystones, siltstones, sandstones, and coals, evident from the serrate pattern on gamma-ray logs. The Puzzle Hole Formation is distinctively coarser grained than the underlying marginal marine/lacustrine Middle Graben Formation. The depositional setting is interpreted as lower delta plain, with occurrence of lagoonal tidal flats, estuaries, tidal channels, bay head-deltas and mouthbars (Munsterman, 2011). Distinctive terrestrial palynofacies in the claystones of the Puzzle Hole Formation contrast with the predominantly marine palynofacies in the Middle Graben Formation claystones.

Overall, the continental units (Lower and Middle Graben formations and Puzzle Hole Formation) in the first Upper Jurassic sequence reflect a gradual marine transgression, partly alternated by tectonically controlled phases of progradation of siliciclastics (Wong, 2007). These progradational phases are reflected in the interfingering occurring within the continental Schieland Group and between the Schieland Group and Scruff Group. The boundary between the Schieland group and the Scruff group is diachronous. Herngreen (2003) argues that the introduction of relatively coarse siliciclastics (including the Puzzle Hole Formation, main Friese Front Member, and the Upper Graben Formation) coincided with the start of the late Cimmerian tectonic phase. However, no supportive evidence for the tectonic nature of this change in facies was provided, which is one of the motivations of this study.

Sequence 2 (Abbink, 2006; Munsterman, 2011), or TMS-2 (Bouroullec, 2018; Verreussel, 2018) spans the Kimmeridgian and Early Portlandian and is equivalent to stage 3b, 3c, and to the lower part of stage 3d (Herngreen, 2003). This sequence is essentially a continuation of the transgressive trend in the first sequence. It is largely comprised by the marine Kimmeridge Clay Formation, of which the oldest part interfingers with the continental lithological formations of the Schieland group (Sequence 1). The **Kimmeridge Clay Formation** is part of the Scruff Group. It comprises silty claystones with thin dolomite streaks. Towards the south, the formation tends to het gradually siltier and sandier. The KCF was deposited in an outer shelf setting where dolomite streaks and intervals with increased organic matter indicate periods of sediment starvation and possibly stagnant water columns. The south to north transition from proximal to distal facies is illustrated by a Tithonian to Kimmeridgian

paleogeographic map (figure 4) published by (Wong et al., 2007) and modified from Ziegler (1990)

In the upper part of sequence 2, the Kimmeridge Clay Formation interfingers with the Skylge Formation (Munsterman, 2011). This formation comprises the Oyster Ground, Terschelling Sandstone, Noordvaarder and Lies Members, that are no longer part of the Friese Front Formation (or Schieland group) because of their restricted marine character (Munsterman, 2011). The Oyster Ground, Terschelling Sandstone and Noordvaarder Members are local sand-rich units within the overall claystone/siltstone dominated Scruff Group. **The Lies Member** consists of bioturbated silty to sandy claystones with locally glauconitic, pyritic and carbonate intervals (Munsterman, 2011). These sediments were deposited in an offshore-shelf environment (Munsterman, 2011). During deposition of Sequence 2, the depositional area widened and incorporated surrounding areas like the Terschelling Basin and the Step Graben. In addition, a clear depocenter shift towards the western basin margin is observed in seismic sections in the area of the Dutch Central Graben (van Wijhe, 1987, Herngreen, 2003).

Sequence 3 is dated as Early Portlandian and is marked at the base by a (regional) unconformity. All late Jurassic basins became incorporated into a greater depositional area by this time. This sequence corresponds to TMS-3 defined by Bouroullec (2018). The Scruff Greensand Fm is connected in the north with the distal Lutine Formation (Munsterman, 2011), which rests unconformably on the Kimmeridge Clay Formation in the north. The Scruff Greensand Formation contains the **Scruff Spiculite Member,** which occurs in the lower part of Sequence 3. This member consists of light green-grey, fine-grained, and glauconitic slightly argillaceous bioturbated bioclastic sands, with abundant spiculites. These were deposited in an (offshore) to shoreface environment (Abbink et al., 2006).

Sequence 4 marks the termination of the Jurassic rift sequence. The entire area was subsequently subjected to subsidence, marked by the transition to the marine Rijnland group, encompassing all previous basins and onlapping adjacent highs. Locally, the transition from Sequence 3 to Sequence 4 is a hiatus.

3. Methods

3.1 Tectonic successions in salt-influenced basins

In order to further refine the tectono-stratigraphic framework and its spatial variability, we use a tectonic succession methodology (Matenco and Haq, 2020 and references therein) that builds upon extensive analysis of rift sequence system tracts and related concepts (e.g., Leeder and Gawthorpe, 1987; Prosser, 1993 among many others). This approach comes from the observation that the fundamental controlling factors governing clastic sequence stratigraphy are fundamentally different from the factors that control rift sequences (see also Martins-Neto and Catuneanu, 2010; Neal et al., 2016). Sequence stratigraphy assumes a control by eurybatic or eustatic movements superimposed on longer time-scale thermal subsidence. However, most sedimentary basins have an initial tectonically driven phase. During such tectonic phases, creation of depositional space is mostly fault-controlled, and sea-level plays a subordinate role.

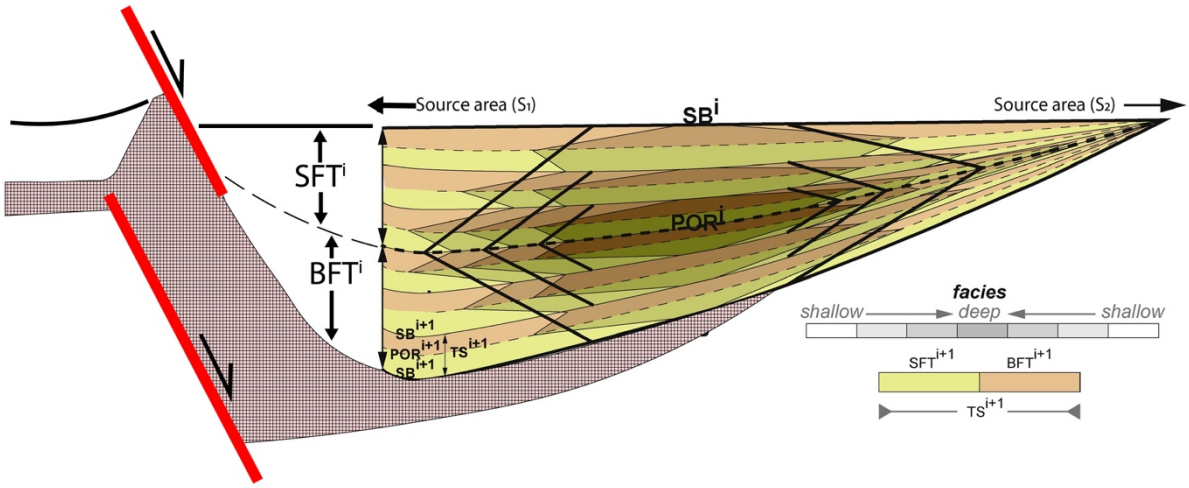

Figure 5. Conceptual idea of the tectonic succession methodology. This illustration indicates higher ($TS1^{i+1}$) and lower (TS1) tectonic successions composed of sourceward migrating and basinward migrating facies tracts. These facies tracts fill accommodation space that is created by local structures. In the Dutch Central Graben such local structures are likely to be combined systems of brittle deformation (faulting) and ductile deformation (salt movement). Modified from Matenco and Haq (2020) and ten Veen (2012).

Models for active rifting systems are commonly subdivided into a rift initiation, rift-climax and post-rift stage (or sometimes as early, climax, late and post-rift stages). The rift initiation is marked by an alluvial phase sourced from the rift axis. As fault offset and thereby subsidence increases, deeper marine facies are established that intercalate with gravity driven mass-wasting deposits close to the fault plane. This is termed the rift climax. The subsequent (early or late) post-rift stage is essentially controlled by a (relative) decrease in subsidence and an increasingly dominant role for sediment supply which results in rapid infill of available accommodation space. These earlier models are in many ways similar to tectonic succession methodology. The tectonic succession methodology (figure 5) relies on two fundamental building units: a sourceward migrating facies tract (SFT) and a basinward migrating facies tract (BFT). The SFT is characterized by high δAS/ δSS (accommodation space creation versus sediment supply) and the occurrence of shallow water facies shifting towards the source of sediment supply. The subsequent BFT is characterized by a low δAS/ δSS and a basinward migration of facies. Together the SFT and BFT comprise a tectonic succession that is bounded by succession boundaries (figure 5). The alternation of these tectonic successions on different scales correspond to distinct phases of deepening or shallowing induced by tectonics, or by any other external forcing factor, such as eustasy or the rate of sediment supply. The temporal scale of such alternations can range from plate tectonic cycles to individual fault movements (Matenco and Haq, 2020). The tectonic succession methodology presents a straightforward and simple framework to categorize the early stages of a rift prior to passive margin development.

Most studies dealing with rift sequence stratigraphy or tectonic succession terminology have been developed for fault-controlled basins. Such models do not cover the decoupling role of salt as a mechanism driving accommodation space (see also ten Veen et al., 2012). Most facies models in rift sequence analysis rely on the asymmetry and the typical topography that is created by fault movements. In the case of the Dutch Central Graben, most of the Jurassic extensional deformation occurred due to reactivation of older sub-salt Permo-Triassic normal faults (ten Veen et al., 2012), with Zechstein evaporites acting as a decoupling layer. This means that basin physiography is expected to be different between salt-influenced and salt-free basins. Only limited studies are available that have documented in detail such variations (Alves et al., 2003; Banham and Mountney, 2013; Bouroullec et al., 2018; Mannie et al., 2016).

3.2 Seismic interpretation, reconstruction and well analysis

3.2.1 First-order seismic interpretation and reconstruction

For a fairly large available dataset, we have used a number of 2D and 3D seismic surveys for a first-order interpretation, of which 2 transects are presented in this study. The northern Section A is spatially juxtaposed against the seismic line NSR 1057 (figure 3), while the southern section B is a composite section of 2D seismic lines (NSR 1053 and NSR 1054) and a 3D seismic survey (figure 4). The composite section is correlated across three wells that enabled a further high-resolution analysis. We have used a classical seismic interpretation approach of mapping reflector terminations, used to interpret faults and unconformities that bound syn-kinematic sedimentary units. Available well data and existing 3D models of the Dutch Subsurface (DGM-diep, version 5, TNO, 2019) are used to infer relative ages of boundaries and sedimentary units that can be correlated across the section. Our first order interpretation and correlation uses the standard NL stratigraphic framework (dinoloket.nl), improved by differentiation of units and facies correlation based on observations in seismics and wells.

The transects A and B are reconstructed and presented in a stepwise evolution (figure 9 - 14). Reconstruction is based on flattening the interpreted unconformities that bound stratigraphic units in Petrel 2019. A flattened seismic section is an estimation of the structural configuration during the moment in geological time that corresponds to the flattened horizon. Note that such a reconstruction gives a first-order approximation, because it does not include the paleo-elevation or paleo-bathymetry, nor it accounts for lateral displacements across various fault or salt structures.

Based on cross-correlation of unconformities, larger panels that give an estimation of the entire section were constructed. In areas where horizons terminate or truncate (due to erosion or non-deposition), the horizons are either extrapolated (mostly in case of erosion) or the estimated structural configuration is clarified by schematic annotation. This was done only for the Jurassic units, since erosion of these units is significant around the basin axis. The additional erosion created by the Cretaceous inversion was not estimated.

3.2.2 Combined high-resolution well and seismic facies analysis

Three wells (F11-01, F11-02, F11-03) were analyzed in higher resolution to describe changes in overall grain size and depositional facies. In combination with seismic facies analysis, this has enabled the detection of basinward migrating (progradational) and sourceward migrating (retrogradational) facies tracts,

In terms of well-logs, we used the standard time-depth correlation and seismic velocities available in DGM-Diep and the VelMod dataset (nlog.nl). We further combined Gamma ray, Neutron, Density and Sonic logs to define distinct trends in lithology. A combined plot of gamma ray and sonic data was used in addition to a combined plot of density and neutron data. We have used a standard approach in well-log sequential analysis that uses primarily gamma-rays for clastic composition, while density, neutron, sonic and electric logs combined with core samples were used to derive lithological content and its variability. High density, neutron porosity and gamma ray activity can lead to misidentifying a glauconitic sand as a shale. For Scruff Group sediments, known to contain significant amounts of glauconite, close inspection of core reports was done to prevent potential errors in determining grain size trends.

Based on careful observation of well log trends, well log facies can be differentiated. These well log facies are used in combination with lithological data based on core reports and core

descriptions (dinoloket.nl), and literature on regional lithostratigraphy, to enable the interpretation of depositional environment and to detect sedimentary cycles. This combined data set was used to define trends/cycles at three different scales: *parasequences, fining or coarsening upwards sets of parasequences and lower order cycles*. All the data was subsequently complemented with a TNO age model based on biostratigraphy reports, available in the DinoLoket database, updated and high-resolution sea-level curves (Haq, 2018, 2014) and an isotope curve (Ogg et al., 2016) to enable a detailed analysis of potential allogenic mechanisms. For Late Jurassic to Lower Cretaceous siliciclastic sequences, an additional high-resolution seismic analysis was performed based on the tectonic succession methodology as described in the methodology section. This analysis was linked to the well analysis in order to distinguish basinward migrating and sourceward migrating facies tracts.

4. Results: seismic interpretation

Our first-order interpretation (figure 7 & 8) separates several distinct seismic units bounded by clear unconformities. Separating unconformities are expressed most strongly around structural features such as salt bodies and faults, but most of them extent quite far laterally, beyond these features. They represent events at the scale of the entire studied area and are therefore suitable to create regional reconstructions. Seismic units have distinctive characteristics that enable correlation across transects (figure 6). The approach here is specifically aimed at building a first-order interpretation. A more detailed analysis of seismic facies and stratal configurations, in combination with analysis of well data, is subsequently performed for the Callovian to Berriasian Schieland and Scruff Groups.

examples (vertical scale is 250 ms)	colour code and name	general characteristics
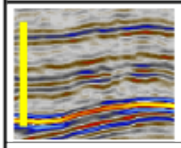	= Cenozoic North Sea Supergroup	highly variable but generally underlain by an exceptionally strong high amplitude reflector
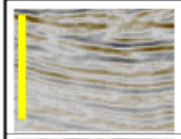	= Cretaceous Chalk	low amplitude, high frequency, fairly continuous reflectors
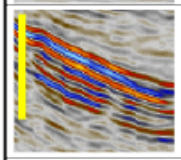	= Rijnland Group	very high amplitude, low frequency, continuous reflectors
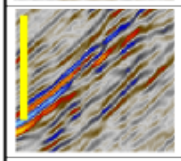	= Schieland & Scruff Group (S1, S2, S3, S4)	high variability in general appearance of reflectors. Further details are provided in the high-resolution combined well and seismic analysis
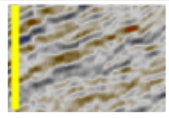	= Posidonia Shale Formation	intermediate amplitude, low frequency, fairly continuous reflectors, slight variability in appearance of reflectors
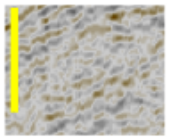	= Altena Group	low amplitude, discontinuous reflectors, chaotic in places
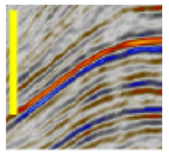	= Triassic	highly variable appearance
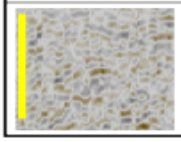	= Zechstein Salt	chaotic, typical for evaporites

Figure 6. Seismic facies units classification scheme for the two transects interpreted in this research (A&B). This classification is specifically aimed to provide a first-order interpretation, followed subsequently by a more detailed analysis of the Upper Jurassic Schieland and Scruff Groups.

4.1 Section A

The northernmost section A (figure 7) is structured by three prominent salt bodies, of which the western- and easternmost bodies delineate the Jurassic basin fill. The Zechstein salt unit, characterized by a typical chaotic, transparent appearance of seismic reflectors, is highly variable in thickness and reaches a depth of 1750 -2000 ms locally, due to halokinesis. It is overlain by a Triassic unit, which shows locally thickness variations and syn-kinematic strata. The Triassic unit is overlain by the Lower Jurassic Altena Group, which is wedge-shaped, relatively uniform in appearance, and thins in both eastern and western directions, attesting to vertical relative movements along both margins associated with salt redistribution. The Altena Group is significantly truncated along the eastern margin, where it is directly overlain by Cretaceous deposits. Along the western margin, the Altena Group pinches out, without being affected much by erosion. It is generally characterized by low frequency, low amplitude reflectors. A differentiation in seismic facies occurs in the upper part of the Altena Group, due to contrasting lithologies in the Posidonia Shale Formation.

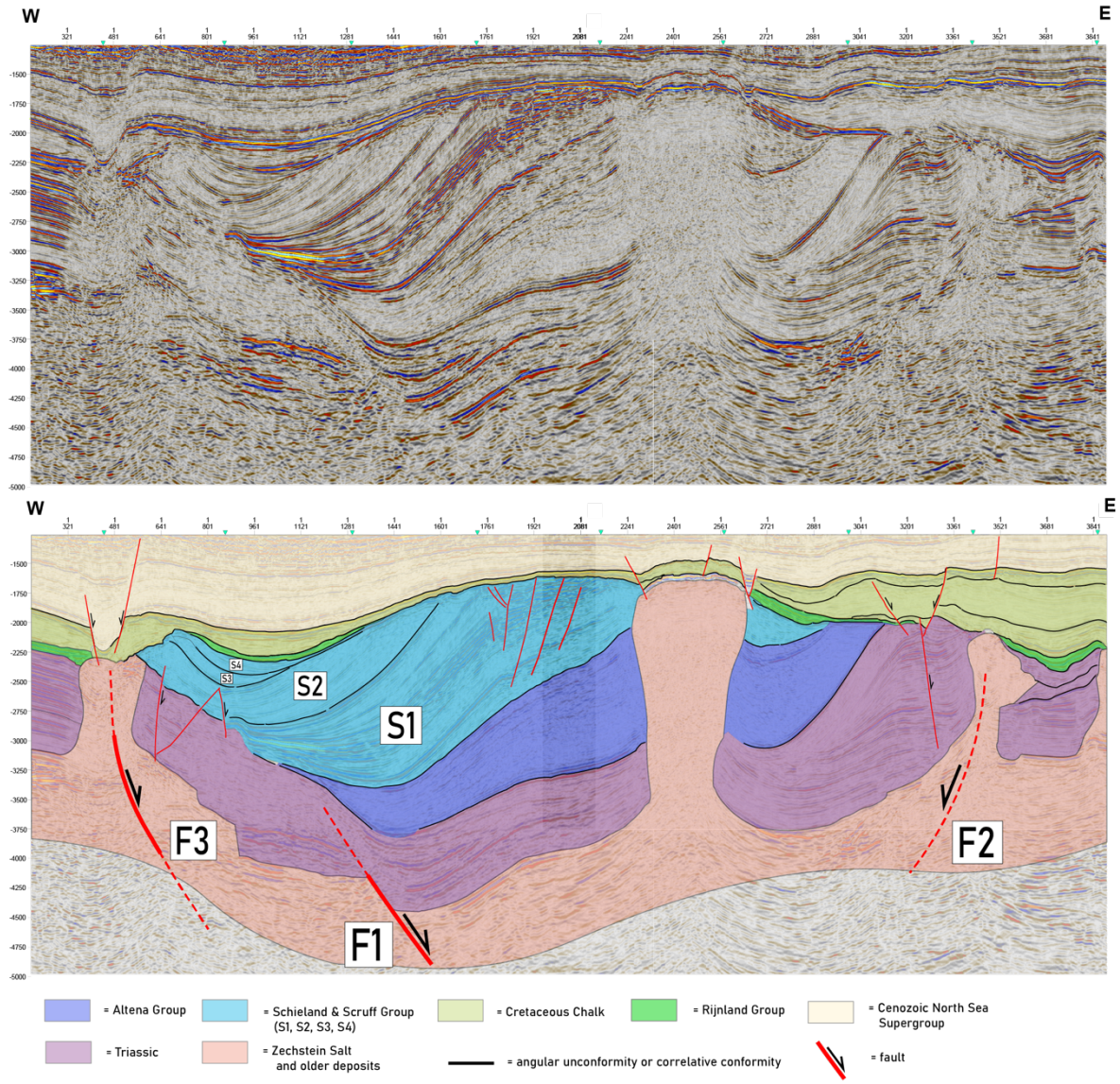

Figure 7. Seismic interpretation of section A. See figure 1 for location. The Schieland and Scruff Group are subdivided into four distinct units (S1, S2, S3, S4). Three main sub-salt faults were interpreted (F1, F2, F3). Dashed lines indicate areas where clear interpretation is hampered.

The Altena Group is separated from the Upper Jurassic by a significant unconformity, recognized over the entire transect. Seismic facies do not change significantly across this unconformity apart from a shift to slightly higher frequency of reflectors. The Upper Jurassic unit (Schieland & Scruff Group) is laterally as well as vertically highly variable in terms of seismic facies. The first-order interpretation of the Upper Jurassic Schieland and Scruff Group is subdivided into 4 units (S1, S2, S3, and S4) separated by laterally extensive unconformities that are strongest around the margins and pass into correlative conformities. These units are characterized by clear depocenters shifts, demonstrating distinct phases of basin nfill.

Unit S1 is a broad-wavelength combined syn- and anti-form, deformed in a similar style as underlying Triassic and Lower Jurassic strata. It is significantly eroded along the center of the basin where it directly underlies much younger Cenozoic strata and it thins towards the western basin margin indicating relative uplift of the margin during deposition. In terms of seismic facies, unit S1 contains significantly higher amplitude reflectors than overlying units S2, S3, and S4. Along the basin center, where strata are strongly folded, small post-depositional faults offset strata of unit S1. Unit S2 oversteps the former western basin margin, and remains roughly equally thick towards the west, although its original depositional extent is not preserved. Towards the east, unit S2 is truncated along the basin axis representing significant removal of strata. The overlying units S3 and S4 represent a change in depositional style from westward thinning sedimentary wedges (S1 & S2) towards eastward thinning sedimentary wedges that are located along the former margin of the basin. Such a basin margin wedge is termed a peripheral salt basin or rim syncline, usually related to a change in salt migration (Trusheim, 1960) and in this case vertical movement of the basin center. The basin infill of S3 and S4 is characterized by low amplitude reflectors with varying frequency, onlapping over the antiform in the center of the basin. Deposition continues with a thin sequence of the Cretaceous Rijnland Group, characterized by high amplitude reflectors, overlain by the Cretaceous Chalk unit, which is present in the entire section but shows strong variation in thickness associated with syndepositional uplift of the basin center. The overlying Cretaceous chalk unit is characterized by low amplitude, high frequency and fairly continuous reflectors. Locally, low-offset faults have affected the Cretaceous and Cenozoic and are rooted in the Zechstein and Triassic around local highs created by salt bodies. The Cretaceous chalk unit is subdivided in the east by angular unconformities, not observed in the western part. The overall geometry of the Chalk unit is in agreement with syn- kinematic deposition during Late Cretaceous and Cenozoic inversion, affecting differently the western and eastern part of the transect.

4.2 Section B

Section B is located several kilometers southwards and bears close resemblance to section A (figure 8). This section is to a large extent affected by the movement of Zechstein salt, which reaches relatively shallow depths due to post-depositional remobilization. The overlying Triassic strata show minor thickness differences, reflector terminations and variable seismic facies evidencing syn-kinematic sedimentation, similar to section A. The Triassic is truncated along the margins and overlain by Cretaceous deposits of the Valanginian Rijnland Group in the east, and Berriasian to Tithonian deposits of the Scruff Group in the west. In the central part of the basin, the Triassic is overlain by the Lower Jurassic Altena Group, pinching out in the west, and truncated in the east. The Altena Group in section B is characterized by low frequency, low amplitude reflectors with a very strong reflector underlying its upper bounding unconformity, resembling the Posidonia Shale Formation. Both Altena and Triassic units are deformed and structured in broad wavelength anti- and synforms, just like overlying Upper Jurassic strata. The Altena Group thins towards the western margin, attesting to relative vertical motion of this margin.

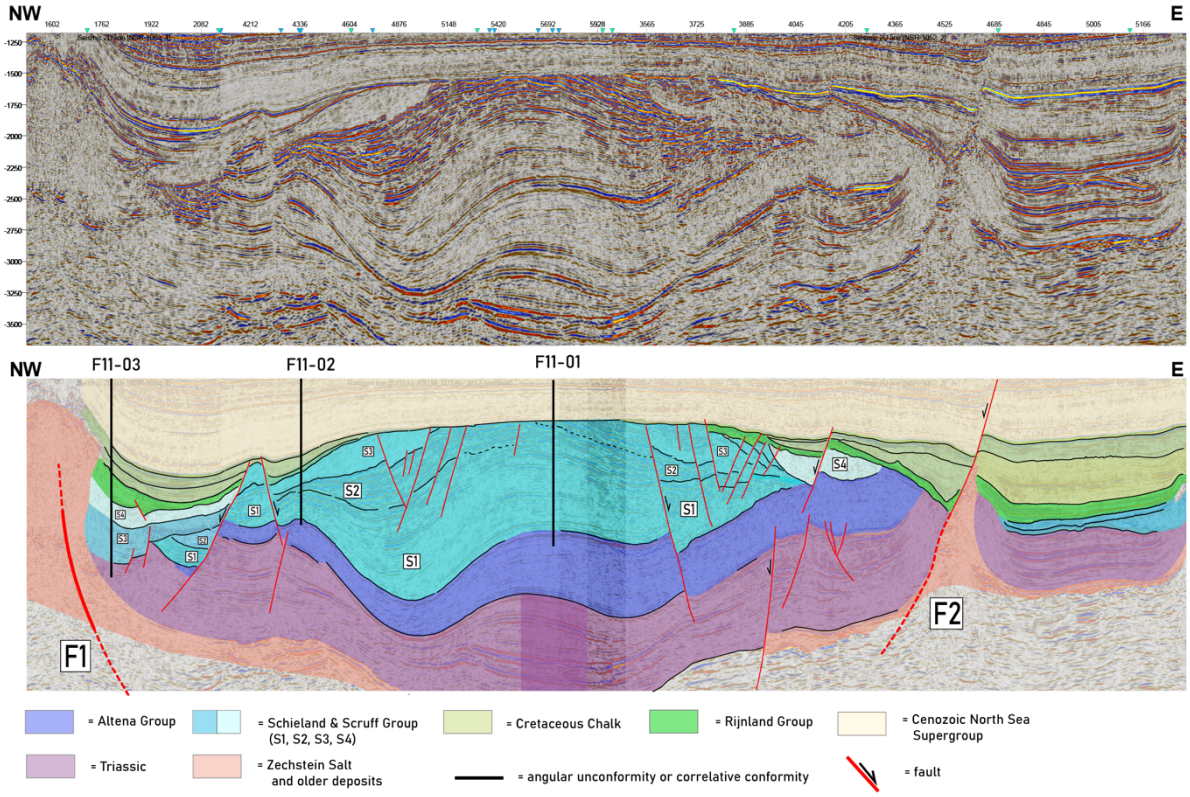

Figure 8. Seismic interpretation of section B. See figure 1 for location. The Schieland and Scruff Group are subdivided into four distinct units (S1, S2, S3, S4).

The units of the Upper Jurassic Schieland & Scruff Groups (S1, S2, S3, S4) are separated from the underlying Altena Group by an unconformity. This unconformity is evident along the margins but changes into a correlative conformity in the center of the basin. When compared with section A, the clear shift of depocenters towards the west is not evident in section B. In the latter, the sedimentary units are equally developed along both margins in terms of thickness and preservation, with some minor differences. The two lowermost units of this interval (S1 & S2) thin towards the basin margins and have a depocenters that coincide roughly with the depocenter of the Altena Group. Unit S1 is dominated by mostly low amplitude reflectors gradually changing into higher amplitude reflectors upwards, whereas unit S2 is solely dominated by high amplitude reflectors. Reflectors in both units are generally discontinuous and affected by post-depositional faulting and folding. In the west, S1 and S2 are affected by a major fault that is rooted in Zechstein salt and decoupled from deeper levels. The upper boundary of unit S2 is marked by a clear angular unconformity and a strong change in seismic amplitude. Both unit S1 and S2 thin towards the eastern and western margins, reflecting continued relative vertical motion of these margins. S3 overlies S2 and is eroded to a large degree along the axis of the basin, while S4 is located solely along the margins and onlaps over the local high that was created by the antiform in the center of the basin, showing a change to rim syncline deposition, similar to observations in section A.

Continued deposition of the Cretaceous is focused along the margins. The Rijnland Group and Cretaceous Chalk Group onlap the adjacent highs and are gradually sedimented over a larger depositional area. Their appearance in terms of seismic facies is similar to the seismic facies described for section A. A clear difference with section A is that the eroded Jurassic block in the basin center is overlain directly by the Cenozoic. No Cretaceous strata are observed here.

5. Results: reconstruction

5.1 Reconstruction of section A

The Jurassic reconstruction of section A (figure 9) is based on flattened unconformities and horizons from the earlier discussed interpretation. The reconstruction of section A comprises three units: the Altena group (figure 9A), the Schieland 1 (Figure 9B) and Schieland 2 (Figure 9C) groups. During deposition of the Altena Group, accommodation space was indirectly created by movement along fault F1 and fault F2. In the flattened section (figure 7A), offset along fault F1 is clearly observed, and affects both Zechstein as well as Triassic strata. Due to the quality of reflectors at this depth, it is not clear whether faut F1 crosses the top of the

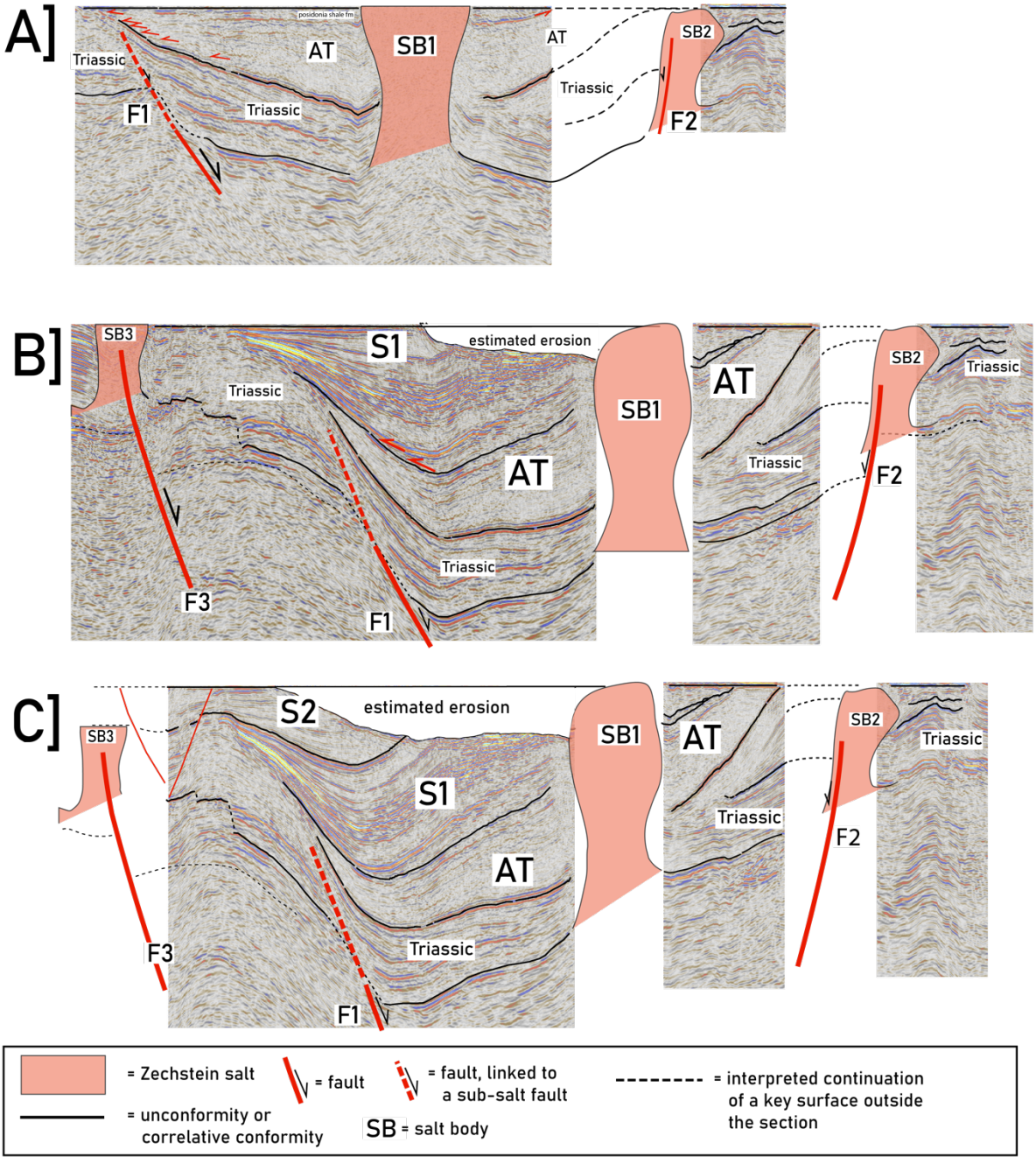

Figure 9. Jurassic structural evolution of section A. A) section flattened on top of the Jurassic Altena Group, B) section flattened on top of the S1 unit, C) section flattened on top of the S2 unit.

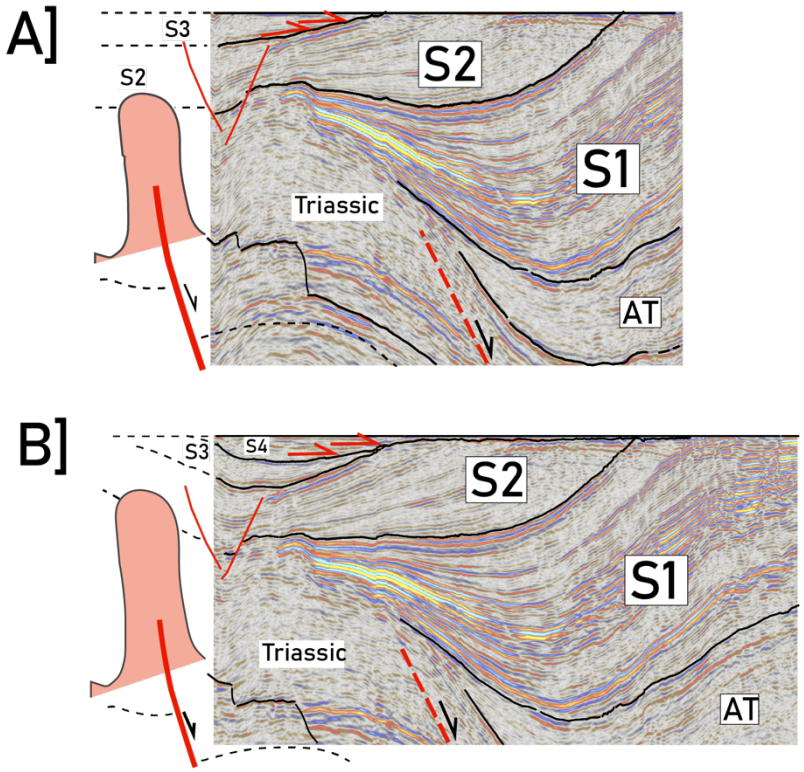

Figure 10. Late Jurassic reconstruction of the western part of seismic section A. The reconstruction illustrates the transition to rim syncline deposition along the basin margin.

Zechstein and links to the Triassic. The Zechstein might have been significantly thin here due to earlier Triassic remobilization. In that case, movement along F1 was hard-linked with the underlying basement and penetrated upwards into the Triassic, indicated in figure 9 by a dotted line (see also ten Veen et al., 2012). The Altena Group thins and pinches out towards the margin and is not affected by fault F1. In the west, it onlaps the Triassic. Offset along fault F2 created accommodation space in the east but was clearly decoupled from deformation in the Triassic and Jurassic overburden. Fault F2 underlies a prominent salt body (SB2) that is not penetrated by upward propagation of fault F2.

Unit S1 (figure 9B) shows a depositional shift towards the west, and a sedimentation area that extends further eastwards than the Altena Group. Accommodation space was created by a large offset along fault F1. This is clearly observed by the sharp contrast in offsets along this fault between flattened sections (comparing figure 9A with 9B). Unit S1 onlaps over the underlying Altena Group and is not affected by any hard-linked faulting. Its deposition is restricted to an area roughly equal to the depositional area of the Altena Group. No clear observation can be made regarding the role of faulting along fault F3 during deposition of S1. Given significant S1 thinning at far distances from F3, coeval faulting was likely minor and most of the created accommodation space was caused by F1, in close combination with salt movement/withdrawal. Unit S2 oversteps previous basin margins and does not pinch-out. It was possibly deposited over a much more extensive area than previous units, reflecting relative tectonic quiescence and flooding of adjacent highs.

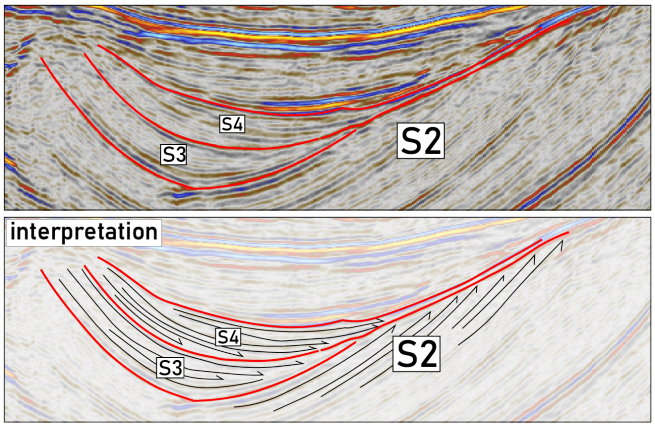

Figure 11. Detailed seismic imagery of the rim syncline at the western margin of the Dutch Central Graben, in section A. The upper section shows an uninterpreted scene and the lower section shows an interpreted version. Stratal organization of reflectors in the interpreted section constrains the timing of axial erosion.

Unit S3 was deposited in a peripheral salt basin phase or rim syncline on the western basin margin. Unit S3 marks a significant change in stratal organization of reflectors (figure 10 & 11). Most reflectors are not separated from overlying units by angular truncation, as observed for S2 and S1. Rather, these reflectors onlap onto the underlying strata and are not significantly tilted. This key observation suggests that by the time of deposition of S3, axial erosion of Jurassic strata deposited in the basin centre occurred, well before the main inversion phases previously defined in the North Sea (Pharaoh et al., 2010). Unit S4 shows no significant change in structuration compared to S3. It onlaps over adjacent highs and extends even further than unit S3, reflecting continued transgression and flooding of the Step Graben (figure 11). Both unit S3 and S4 do not show clear thinning towards the western margin. This indicates that sedimentation occurred over the adjacent plateau, extending further than during the more restricted phase of deposition of the Altena Group and the Callovian to Kimmeridgian Schieland Group (S1 and S2). Deposition of unit S3 and S4 was not affected by faulting. The strong onlap of these units onto the antiform in the basin center suggests that deposition was controlled by long-wavelength deformation and gradual salt withdrawal along the margins rather than hard-linked or soft-linked fault movements.

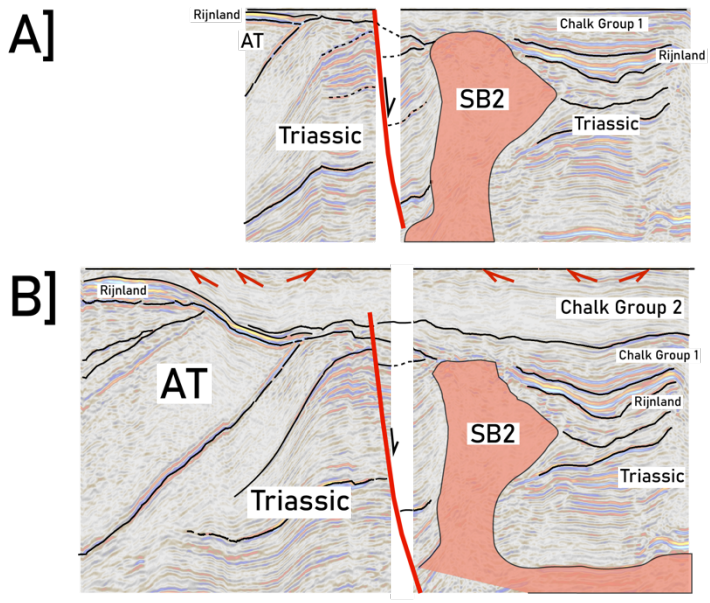

Figure 12. Evidence for Cretaceous inversion in the eastern part of section A. The section is limited to the eastern margin because here, truncation of Cretaceous strata is strongest.

Further structural reconstruction of section A (Rijnland Group and Chalk Group, figure 12) leads to two main observations: First, further transgression and expansion of sedimentation onto all previous structural highs or areas of non-deposition is evident from very prominent onlap of strata. Second, two prominent unconformities (both the topmost boundary of Chalk group 1 and Chalk group 2) indicate structural inversion of Cretaceous strata (figure 12). In particular, the uppermost boundary (above Chalk Group 2) shows very prominent angular truncation at the top of the unit. Such erosion probably resulted from uplift during structural inversion. The signature of Cretaceous inversion is characterized by relatively gentle angular truncation that is widespread in the area, in contrast to Jurassic axial erosion which is focussed mainly on the basin center and created very strong angular truncation.

5.2 Reconstruction of section B

The structural evolution of Section B shows similarities to section A. The Early Jurassic Altena Group thins towards both basin margins (figure 13A). Some minor faulting locally offsets the Altena Group strata in the lower part of the unit. Although the driving mechanism is not fully clear, given the thinning towards both margins, the accommodation space was likely created by continued salt-withdrawal from the graben center, possibly linked to sub-salt faulting in the west and east (fault F1 and F2 in figure 13). In addition, passive thermal subsidence might have played a role during Early Jurassic basin fill. The Altena group is overlain by the first unit of the Schieland Group (S1, figure 13B). This unit reaches further westward than the Altena group, overstepping the Early Jurassic basin margin in the west. It shows major thickness difference across the section and onlaps strongly over the Altena Group, especially in the east. This strong onlap suggests that the Altena Group and underlying units were probably tilted and eroded significantly prior to the deposition of S1, as can be seen in the eastern part of the transect. The accommodation space creation during deposition of S1 was likely caused by sub-salt faulting and associated salt withdrawal (faults F1 and F2). During continued subsidence and deposition of unit S2 (figure 13C), a normal fault formed in the western part of the section (F3). The onlap pattern of unit S2 is particularly strong around the footwall of fault F1. During these times, the activity of fault F1 ceased, deposition overstepped the basin margin in the west, and several small normal faults were formed at the flank of the thick Jurassic succession in the basin center. These faults do not generally root in deeper salt layers but terminate in the Jurassic sequence. Their formation is related to the onset of basin center uplift and a gradual shift of the deposition towards its margins, in a similar way as observed for section A. Furthermore, S3

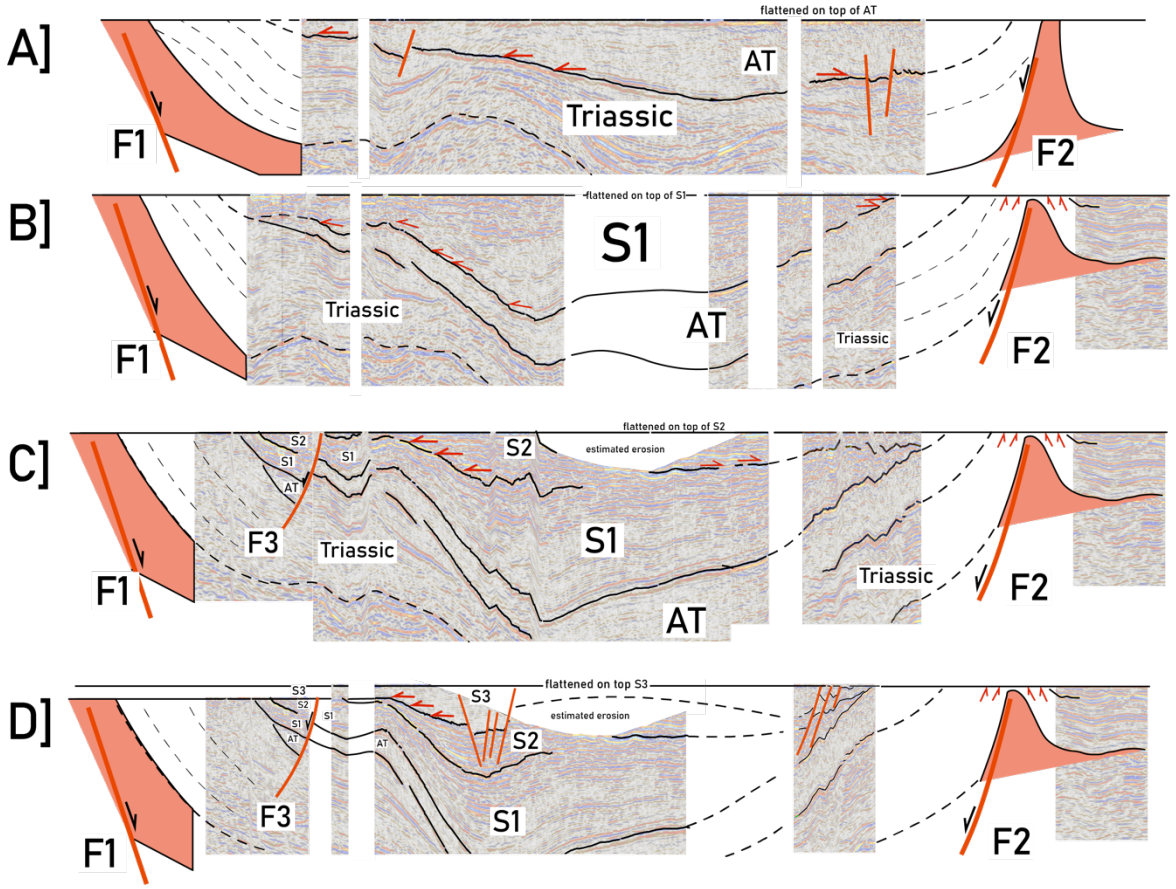

Figure 13 Reconstruction of the Schieland Group in section B. A) section flattened on top of the Altena Group, B) section flattened on top of unit S1, C) section flattened on top of unit S2, D) section flattened on top of unit S3

unit shows no clear pinch-out towards the west, indicating that basin margin faults were not active and deposition could extend and reach adjacent highs.

The Schieland and Scruff Groups are overlain by the Rijnland Group, which has a distinct seismic facies of high-amplitude continuous reflectors, recognized across the entire section. Deposition of the Rijnland Group (figure 14A) occurred during relative tectonic quiescence and gradual transgression, evident from onlap of Rijnland Group sediments over local highs. The top of the Rijnland Group does not show significant truncation, which means that it predates Cretaceous structural inversion. The Rijnland Group is overlain by the Chalk Group. Similar to section A, the eastern part of the seismic section shows greater differentiation within the Chalk Group. Figure 14B shows a detailed flattened section of this eastern part of section B. The Chalk Group onlaps over the underlying Rijnland group, especially onto the footwall of fault F2 and the basin axis, to the west. Chalk Group 1 is also strongly truncated at the top and shows a clear thickness difference across fault F2.

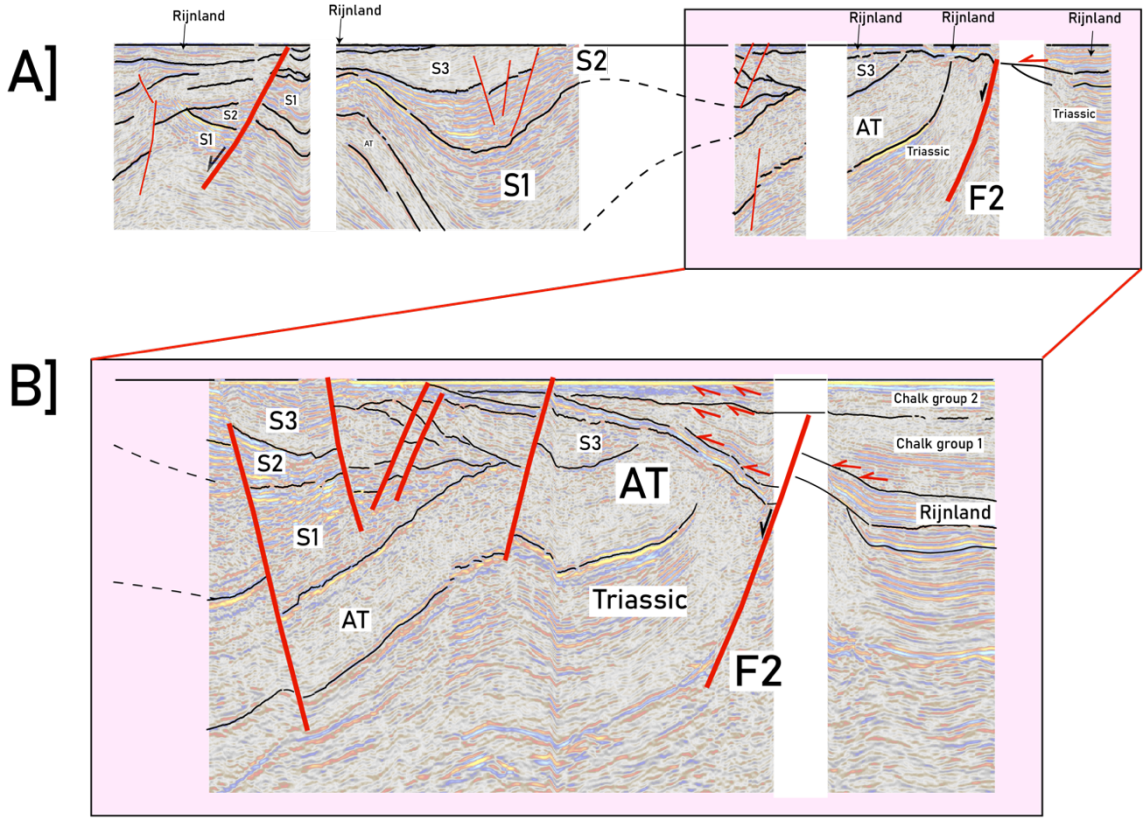

Figure 14. Deposition of Cretaceous Rijnland and Chalk Groups in section B. In 14A the entire transect is depicted flattened on the upper boundary of the Rijnland Group. Section 14B shows a zoomed in version of the eastern part of the transect where inversion of the Chalk Group is obvious.

6. Results: well analysis

6.1 Well log facies

For the analysis of wells F11-01, F11-02, and F11-03 (penetrating seismic section B), a comprehensive well log facies classification scheme was made (figure 15). Well log facies 1 has low GR values and a subtle serrate well log pattern, without very distinct trends or cycles, apart from occasional subtle coarsening upward trends. Well log facies 2 is characterized by rapid alternation between high and low GR values but is on average dominated by low values. Locally, this facies is organized in coarsening upward trends with distinct small block-shaped intervals at the bottom. Well log facies 3 contains similar alternations between low and high GR values, but variations are more gradual and mostly characterized by coarsening rather than fining upward trends. Well log facies 4 is in most aspects similar to well log facies 1, apart from several abrupt and pronounced changes to very low GR values and relatively high-density values, indicative for coal. Well log facies 5 has a highly serrate well log pattern reflected in both GR as well as density. Some intervals have low GR values coinciding with high density

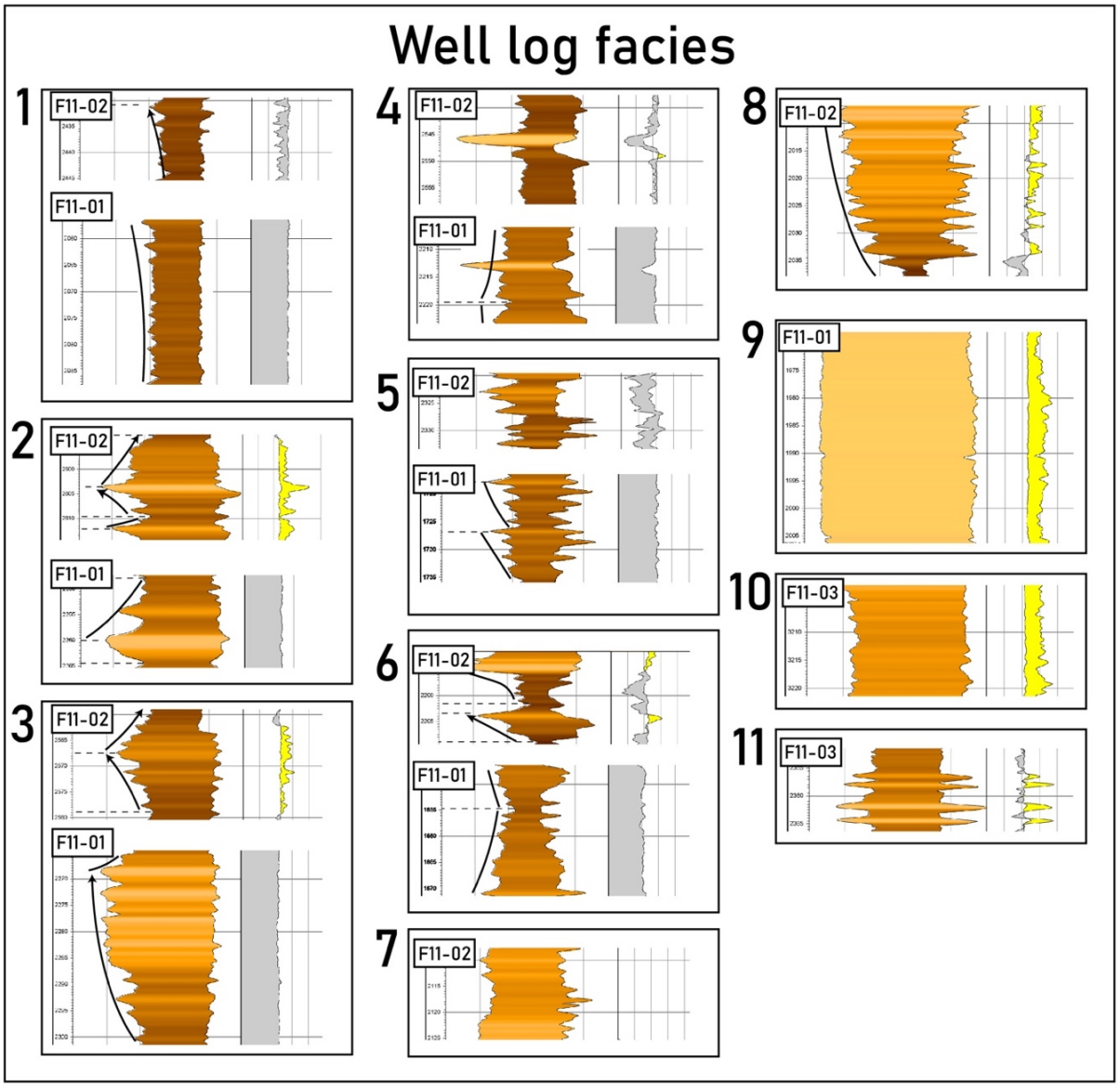

Figure 15. Well log classification scheme used for the interpretation of wells F11-01, F11-02, and F11-03. Some well log facies have a different expression in different wells. This can be due to mud-drilling influencing the well log signal. Also, the typical thickness of a parasequences differ between the two wells. For the representative facies, the log on the left is a combined gamma ray and sonic log whereas the log on the right is a combined neutron and sonic log.This is the same for the wells depicted in figure 16, 17, and 18.

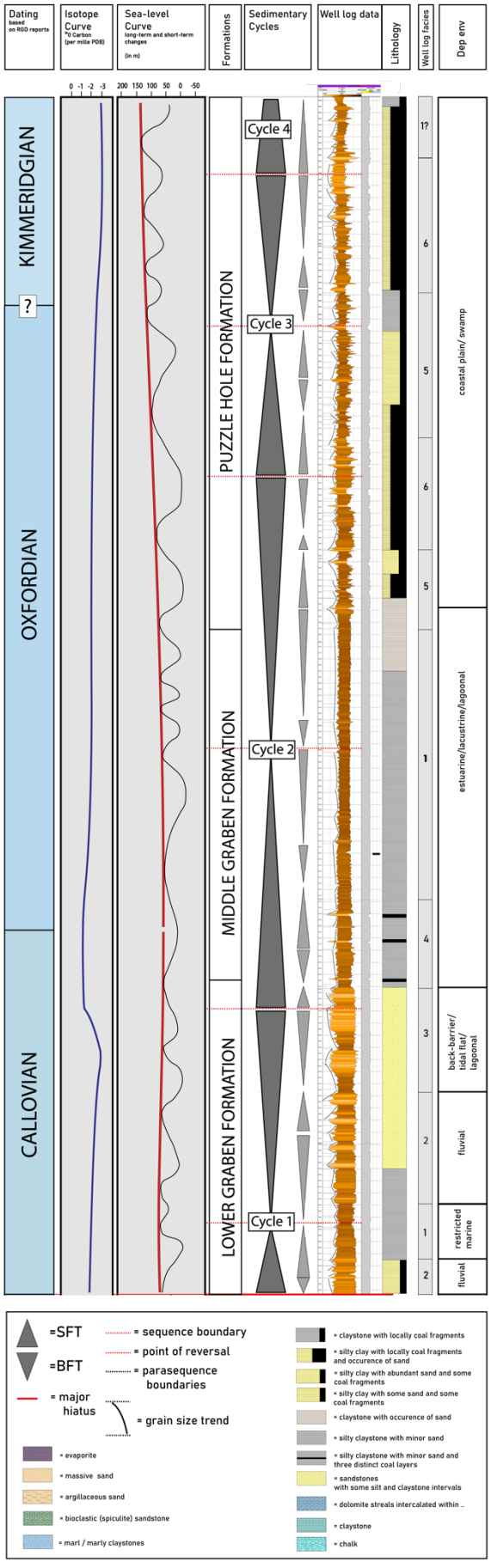

values, which indicates presence of coal seams or layers, although not as abrupt and thick as observed for well log facies 4. Well log facies 6 bears close resemblance to well log facies 5 but contains, on average more intervals with low GR values, and alternations do not occur as rapidly. Well log facies 7 is used for a distinct interval in well F11-02 that only contains gamma ray and density data. Well log facies 8 occurs in the transition to Cretaceous Chalk and contains a thick very clearly coarsening upward parasequence with smaller serrate trends within this parasequence. Well log facies 9 is observed in both F11-01 and F11-03 and has the lowest GR values observed in the entire well log. These high values reflect limestone/chalk lithological composition. Well log facies 10 has relatively low GR values that do not alternate strongly but rather fluctuate subtly over longer intervals. Lastly, well log facies 11 has typically low GR values but strongly alternates with thin streaks that have low GR and low density. These reflect either thin sand intervals or dolomite intervals.

6.2 Well F11-01

Well F11-01 is dominated by fluvio-lacustrine deposits (belonging to the Lower Graben Formation, Middle Graben Formation and Puzzle Hole Formation) and contains three lower order sedimentary cycles, reflected in grain size trends, well log facies, and interpreted depositional environment (figure 16). These cycles can be subdivided into higher-order cycles, and further into individual parasequences. Our focus will be on the lower-order trends and cycles, since these have the appropriate scale to be correlated to seismic data

Figure 16. Well log analysis of F11-01. The log contains several data sets: gamma ray, neutron, sonic and density logs, generalized lithological column based on well reports, biostratigraphic dating (based on reports by the Rijks Geologische Dienst, available at DinoLoket), isotope curve (Ogg et al., 2016), sea-level curve (Haq, 2018, 2014), formation and member names (dinoloket.nl), lower and higher order sedimentary cycles and parasequence trends. The well log facies were assigned to the intervals using the well log classification scheme of figure 15. The depositional environment was interpreted based on a combination of characteristic well log facies, lithology and available literature on the given lithostratigraphic formation or member (Abbink et al., 2006; Munsterman et al., 2012).

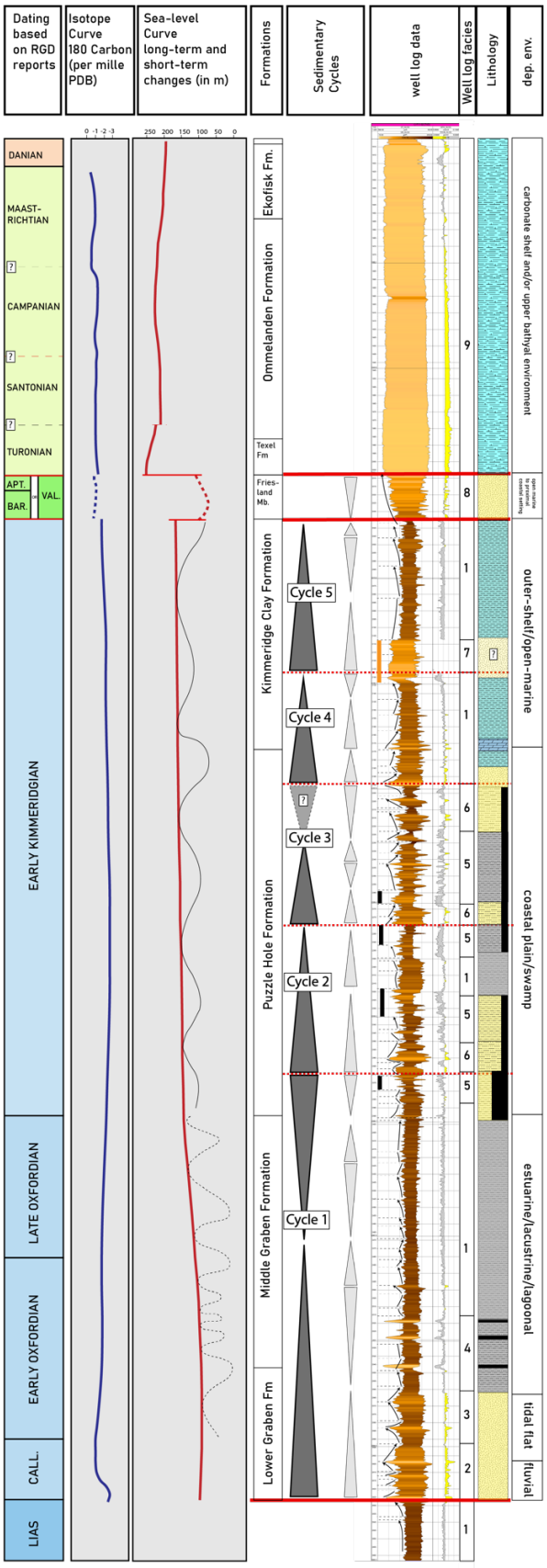

Figure 17. Well log analysis of F11-02. Legend is provided in figure 16. Detailed description and reference of data used are given in the caption of figure 16. Legend is also included in figure 17.

and because our focus lies on allogenic forcing rather than the autogenic parasequence formation.

The lowermost part of Cycle 1 is only observed in well F11-01. These sediments are exclusively deposited in the basin center during a period when later basin margins were not yet reached. Cycle 1 coincides entirely with the Callovian Lower Graben Formation and contains a transition from sand-rich lithologies (well log facies 2) to a clay-rich lithology (well log facies 1) and back to a more sand-rich lithology (well log facies 2 and 3). In this transition, well log facies 2 is characterized by an alternation of sands, silts, and shales occurring in fining upward trends, often with a thin 3 to 4 m block-shaped coarse-grained interval at the bottom (figure 15 & 16). These trends likely result from the formation and lateral migration of fluvial (or deltaic) channels and their subsequent infill. They are commonly observed in other continental/fluvial systems penetrated by well logs. Similar observations and interpretations were made for fluvial sandstones of the Bajocian to Bathonian Bryne Formation in the Danish equivalent of the Dutch Central Graben (Andsbjerg, 2003). The overlying fine-grained facies (well log facies 1) has a subtle serrate pattern without distinct trends, probably resulting from sedimentation in sediment-starved lacustrine to marginal marine areas, without strong clastic input. The upper interval of Cycle 1 in well F11-01 is sand-rich and shows a transition from well log facies 2 to well log facies 3. Well log facies 3 is markedly different, contains thicker individual parasequences with coarsening upward trends rather than fining upward trends. NLOG reports on detailed lithostratigraphy suggests that these deposits were influenced by tides.

Cycle 2 (figure 16) overlaps with the Oxfordian to Callovian Middle Graben Formation and the Lower part of the

Oxfordian Puzzle Hole Formation. Its lower part contains one sand-rich parasequence, similar in lithology and well log facies to the uppermost part of cycle 1. This parasequence is thinner and has, on average, a lower relative GR signal than the underlying interval. It is overlain by a unit with well log facies 4, characterized by thick distinct coal layers, intercalated with intervals that have high GR values and a subtle serrate well log pattern, similar to well log facies 1. On top of this, a thick interval dominated solely by claystones and devoid of any sand is observed, typical for the Middle Graben Formation (well log facies 1). This transition from facies 3 to 4 to 1 represents a fining upward trend on a lower-order scale. The middle interval with well log facies 1 shows, on the scale of parasequences, subtle coarsening upward trends. The uppermost part of cycle 2 is a gradual transition to more coarse-grained lithology, and lower GR signals, coeval with the transition from Middle Graben Formation to Puzzle Hole Formation. The lithology becomes increasingly dominated by sandy claystones, intercalated with coal layers. The well log signal of the upper part of cycle 2 is characterized by well log facies 5 and 6.

Cycle 3 (coinciding with the Oxfordian to Kimmeridgian Puzzle Hole Formation) is slightly more ambiguous in terms of clear lower-order trends. However, a close analysis and distinction between well log facies enables clarification of dominant trends. The lower part of cycle 3 is a transition from well log facies 6 to 5, right above cycle 2. It coincides with a lithological transition from silty claystones containing abundant sand, towards an interval dominated by claystones and occasional coal fragments. Above this, grain size increases again and well log facies changes to facies 6, reflecting a coarsening trend. An overlying short part of a possible fourth cycle is recognized just below the major unconformity that separates the Oxfordian to Kimmeridgian sequence from overlying Cenozoic deposits. Sedimentary cycles in well F11-01 have a typical periodicity of 3 to 5 Ma.

6.3 Well F11-02

F11-02 shows similar trends in well log signal and lithology. A major difference when compared with F11-01 is that the average sedimentation rate is lower. Sedimentary cycles and parasequences are often thinner and more condensed than their equivalents in well F11-01.

The first Callovian – earliest Kimmeridgian lower-order Cycle 1 observed in F11-02 encompasses the Lower Graben Formation, the Middle Graben Formation and the lowermost part of the Puzzle Hole Formation. It has a sand-dominated base, with an upwards transition from well log facies 2 to well log facies 3. The first interval, dominated by well log facies 2 is characterized by a strong alternation of sands, shales and silts, and mostly devoid of coals, resembling closely the observations from intervals with similar well log facies in F11-01. The alternations in this interval are organized in fining upward parasequences with meter scale block-shaped intervals at the bottom. These are overlain by a sandy interval with thicker coarsening upward parasequences, dominated by well log facies 3. Directly above that, mostly claystones occur, intercalated with three thick coals layers, followed by an interval completely dominated by clay and silt, and devoid of any sand and coal. These fine-grained facies are characterized by well log facies 1. The claystones gradually become sandier towards the top of this first cycle, coinciding with the transition to the Puzzle Hole Formation. Cycle 1 is overlain by Early Kimmeridgian Cycle 2 which is dominated by sands, shales, silts and coals. Overall, it shows a gradual fining upwards trend, in a transition from well log facies 6, to 5, and eventually to well log facies 1. The strong serrate pattern, resulting from strong alternation of lithologies is similar to the Puzzle Hole Formation observed in F11-01. The upper part of cycle 2 lacks a coarsening upward trend but is instead abruptly overlain by the first sandy interval that belongs to cycle 3.

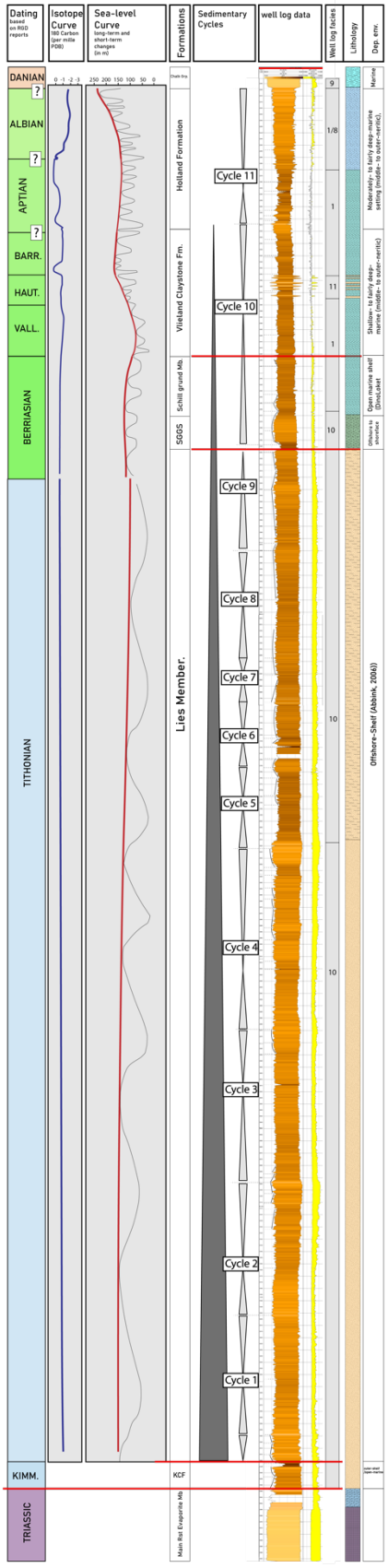

Figure 18. Well log analysis of F11-03. Detailed description and reference of data used are given in the caption of figure 16. Legend is included in figure 16

Cycle 3 belongs again to the Early Kimmeridgian Puzzle Hole Formation. It is a continuation of the serrate well log pattern that is observed in the entire Puzzle Hole Formation. Its lower part is an abrupt change to a sand-rich lithology. Cycle 3 contains an upward transition from well log facies 6, characterized on average by lower GR signals, towards well log facies 5, characterized by higher GR signals, but sometimes alternated with thin sand layers, towards a sequence with well log facies 6, that is predominantly sandy. Cycle 4 starts with an abrupt transition to a sandy interval. This changes upwards into a sequence dominated by claystones and locally intercalated with dolomite streaks, attesting to increased marine influence. The upper part of Cycle 4 and Cycle 5 belong to the Kimmeridge Clay Formation. Overall, the lower-order trend in Cycle 4 is fining upwards and lacks a coarsening upward trend in the upper part. Cycle 5 corresponds to the upper part of the Kimmeridge Clay Formation. Its lower part is a distinctive block-like interval with low GR values, that lacks lithological data but is most probably a sand-rich interval, given the GR values. It is abruptly overlain by a claystone interval dominated by high GR values characteristic for well log facies 2. The Jurassic sedimentary cycles of F11-02 have a typical periodicity of 2 to 5 Ma.

The Jurassic siliciclastics of well F11-02 are, in contrast to F11-01, directly overlain by Cretaceous deposits, separated by an erosional unconformity. The first unit corresponds to the Friesland Member. Biostratigraphic dating available on DinoLoket does not give exclusive evidence for its age. Suggested age models indicate a Barremian to Aptian age or a Vallanginian age. This unit is sand-rich and its well log signal shows a well-developed coarsening upward trend. The Friesland Member is separated by an unconformity from overlying Cretaceous strata. These overlying strata belong to the Cretaceous Chalk Group (Texel Fm., Ommelanden Fm., and Ekofisk Fm.,) They have a quite uniform appearance in terms of well log signal as well as lithology. Its GR signal is very low, and its lithology is exclusively chalky, with occasional variations in siliciclastic input.

6.4 Well F11-03

Well F11-03 covers a Tithonian to Danian interval, that is for the largest part absent in the other two wells. It penetrates the western rim syncline in section A. It is markedly different in well log response and lithology than F11-02 and F11-03. The Jurassic here directly overlays Triassic evaporites from the Main Röt Evaporite Member

(with characteristic low GR values), separated by an unconformity. Above the Triassic, a small interval of Kimmeridge Clay Formation (dated Kimmeridgian) is present, also reported by other literature that uses F11-03 (Bouroullec et al., 2018). It is sandy and it has a low GR signal. The Kimmeridge Clay Formation is overlain by a 800 m succession that is known as the Lies Member, a lateral, more proximal equivalent of the Kimmeridge Clay Formation (Munsterman, 2011). It is expressed in well F11-03 by relatively low GR values. In terms of lithology, it is dominated in the lower part by sands with a varying degree of clay content, in cyclic trends (Cycle 1 – 4) Towards the top, above a stratigraphic level of 2815 m, the second part of the Lies Member is clearly more argillaceous than the lower part and shows, similar to the lower part, cyclic trends in grain size (Cycle 5 – 9). These observations from well log data are supported by the DinoLoket lithological reports. The Lies Member comprises nine sedimentary cycles that range in thickness between 50 m and 150 m. The expression of these cycles in well logs is rather subtle, reflecting variations in clay-content throughout the interval. Their periodicity is typically around 0.8 Ma, roughly equal to the duration of 3rd order sea-level fluctuations.

The Lies Member is separated by an unconformity from two formations. The first formation is the Scruff Spiculite Member, a bioclastic sandstone with spicules as the main framework constituent, and with relatively low GR values. The upper part of the Scruff Group is represented by the Schill Grund Member which contains predominantly claystones with well log facies 1. Another unconformity separates the Scruff Group from the Rijnland Group, comprising the Vlieland Claystone Formation, and the Holland Formation. The Vlieland Claystone Formation contains mostly claystones with high GR values and is interrupted by an abrupt occurrence of 6 to 7 intercalated sandstone layers. The overlying Holland Formation is dominated by clay and marl and shows a gradual decrease in GR values, caused by an increase in carbonate content. The Scruff Spiculite Member, the Schill Grund Member and the Vlieland

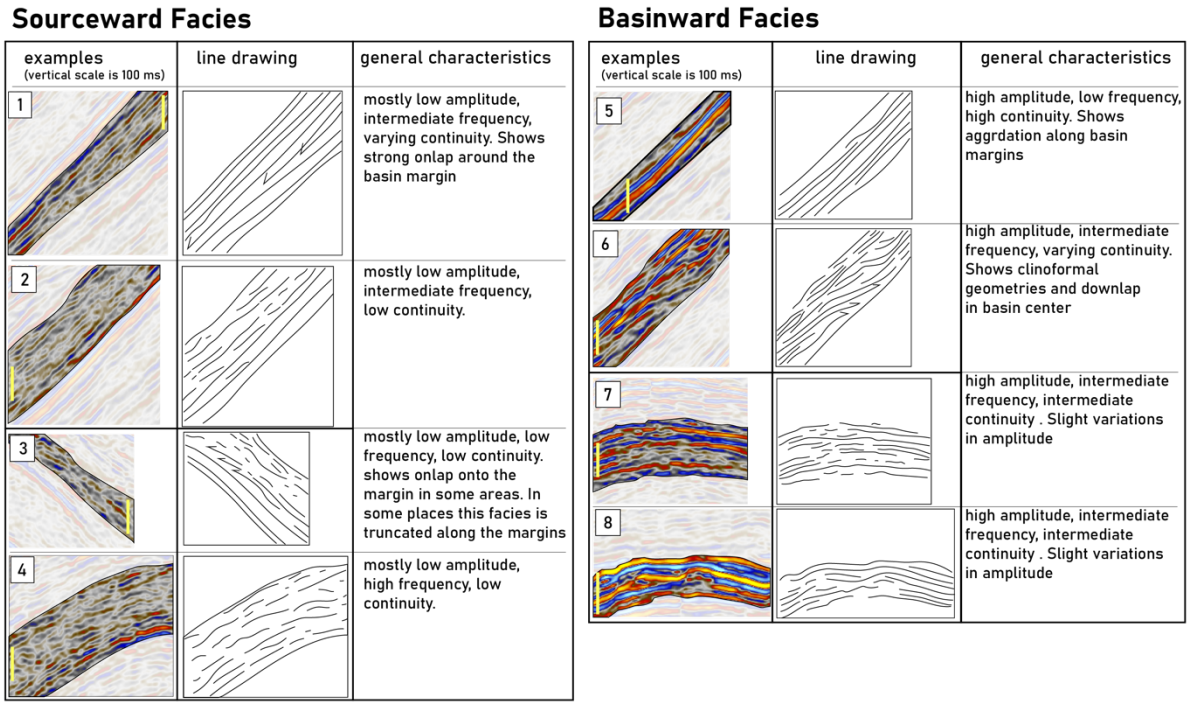

Figure 19. Seismic facies units and their grouping used for high resolution analysis of Upper Jurassic to Lower Cretaceous strata in section A and section B. Sourceward migrating facies tracts and basinward migrating facies tracts together form tectonic successions. Their typical appearance and co-occurrence can vary locally. These variations are described in more detail in the description of the specific sections.

Claystone Member together constitute a sedimentary cycle, comprising a fining upward and coarsening upward trend (Cycle 10). The Holland Formation represents one trend in which the bottom is dominated by claystones, and where lithology gradually increases in carbonate content, with a top dominated by marl and chalk (Cycle 11).

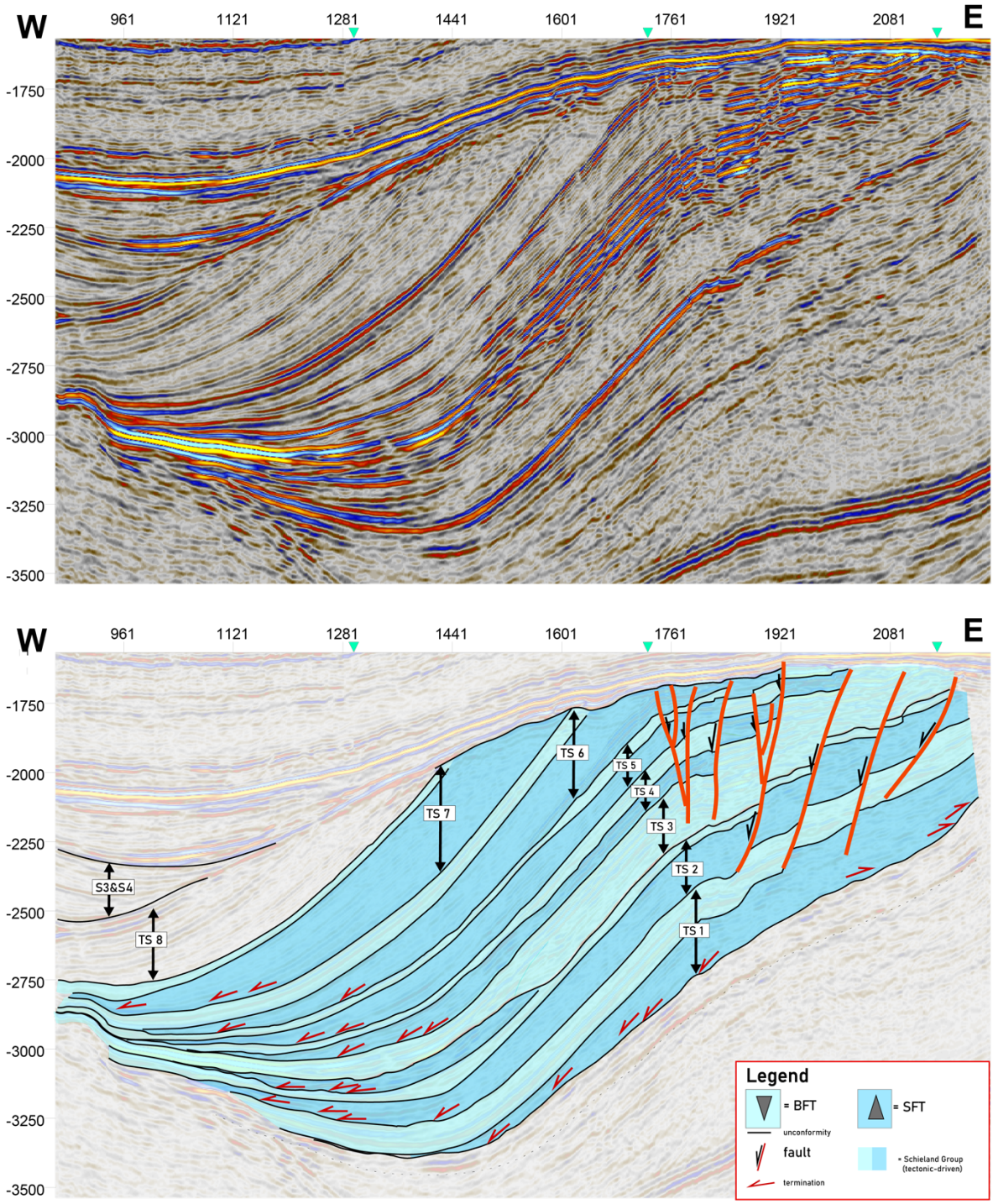

Figure 20. High resolution interpretation of the Upper Jurassic to Lower Cretaceous of section A, without well control. This sequence can be subdivided into tectonic successions that have characteristic signatures in seismics. For this subdivision, the well log classification scheme in figure 15 and the seismic facies classification scheme in figure 19 are used.

7. Combined seismic and well analysis

7.1 High resolution seismic facies analysis

The well analyses of F11-01, F11-02, and F11-03 are combined with an analysis of tectonic successions in order to derive a quantitative tectono-stratigraphic evolution of the Upper Jurassic to Lower Cretaceous Schieland and Scruff Groups. The combined analysis of lithological trends expressed in well logs and stratal configurations of reflectors enables to construct a seismic facies model that defines both basinward migrating as well as sourceward migrating facies tracts (figure 19). Such a model can be further extended to define trends in areas without well control and to convert these trends into lithofacies predictions.

Seismic facies units characterize facies tracts that make up tectonic successions (Matenco and Haq, 2020). Sourceward migrating facies often onlap over underlying strata. They are often characterized by reflectors with low amplitude, relatively high frequency and a varying degree of continuity. The low amplitude of reflectors in the basinal parts of sourceward migrating facies is created by the dominance of shales and the lack of strong lithological contrasts. Amplitude of reflectors are typically higher near the margin attesting to the presence of coarser more proximal facies. In basinward migrating facies, strata show no clear onlap geometries around basin margins and instead are commonly aggradational, especially in the northernmost section A (figure 20). In some cases, the basinward migrating facies tract shows downlap and clinoformal geometries. Such geometries are only observed where resolution of the seismics match a high sedimentation rate. The typical high amplitude of basinward migrating facies tracts results from the frequent occurrence of lithological contrasts between sands, silts, shales and often coal layers.

7.2 Combined well and seismic analysis of section A

Within the entire data set that was used for this research, section A (figure 20, NSR 1057 direction) shows the thickest and most complete sequence of Upper Jurassic Schieland Group siliciclastics within the area. Its high sedimentation rate, resulting in good resolution of facies units, combined with an absence of strong truncation makes it ideal to apply our novel seismic facies model.

Eight tectonic successions are recognized in the detailed high-resolution interpretation of the Upper Jurassic in Section A (figure 20). Many of the distinctive elements of different facies tracts that are described in the seismic facies table are recognized in this interval. The lowermost tectonic succession directly overlies the Lower Jurassic Altena Group, overlying a marked erosional unconformity that can be recognized laterally. The sourceward migrating and basinward migrating facies tracts are equally thick and display the typical characteristics defined in figure 19. The basinward migrating facies tract extends further westwards and has a distinctively high amplitude reflectors configuration. The overlying tectonic succession has a relatively thick sourceward migrating facies tract but a thinner basinward migrating facies tract, which is characterized by markedly higher frequency reflectors than observed in the first tectonic succession. The third tectonic succession is characterized by a thin, laterally restricted sourceward migrating facies tract, which is overlain by a much thicker, very pronounced basinward migrating facies tract. In the more central parts of the basin, this facies tract displays clinoformal reflectors and apparent onlaps that are in fact tilted downlaps. These facies correlate laterally to reflectors that show mostly aggradation near the margin of the succession and extend far westwards, in contrast to sourceward migrating facies tracts. This extension means a large part of the former western part of the basin has been significantly removed by the subsequent erosion. This westward extending BFT is dominated by high amplitude reflectors. The two overlying tectonic successions (TS 4 and TS 5) are both thinner than TS 3

and have typically thinner BFT's compared to the SFT's. The final three TS's (TS 6, 7 and 8) have even thicker SFT's, alternated with thin high-amplitude BFT's. they also encompass a larger depositional area and flood the former basin margin. A particularly interesting observation in section A is the apparent continuous alternation between facies tracts, reflecting cyclic alternation of accommodation space creation and subsequent infill.

7.3 Combined well and seismic analysis of section B

The Upper Jurassic basin infill of section B can be closely correlated to well log patterns in well F11-01, F11-02, and F11-03. Separated by a regional unconformity, the Upper Jurassic Schieland Group overlies the Altena Group, and can be subdivided into tectonic successions. Tectonic succession 1 is relatively thin and its lower sourceward migrating facies tract is

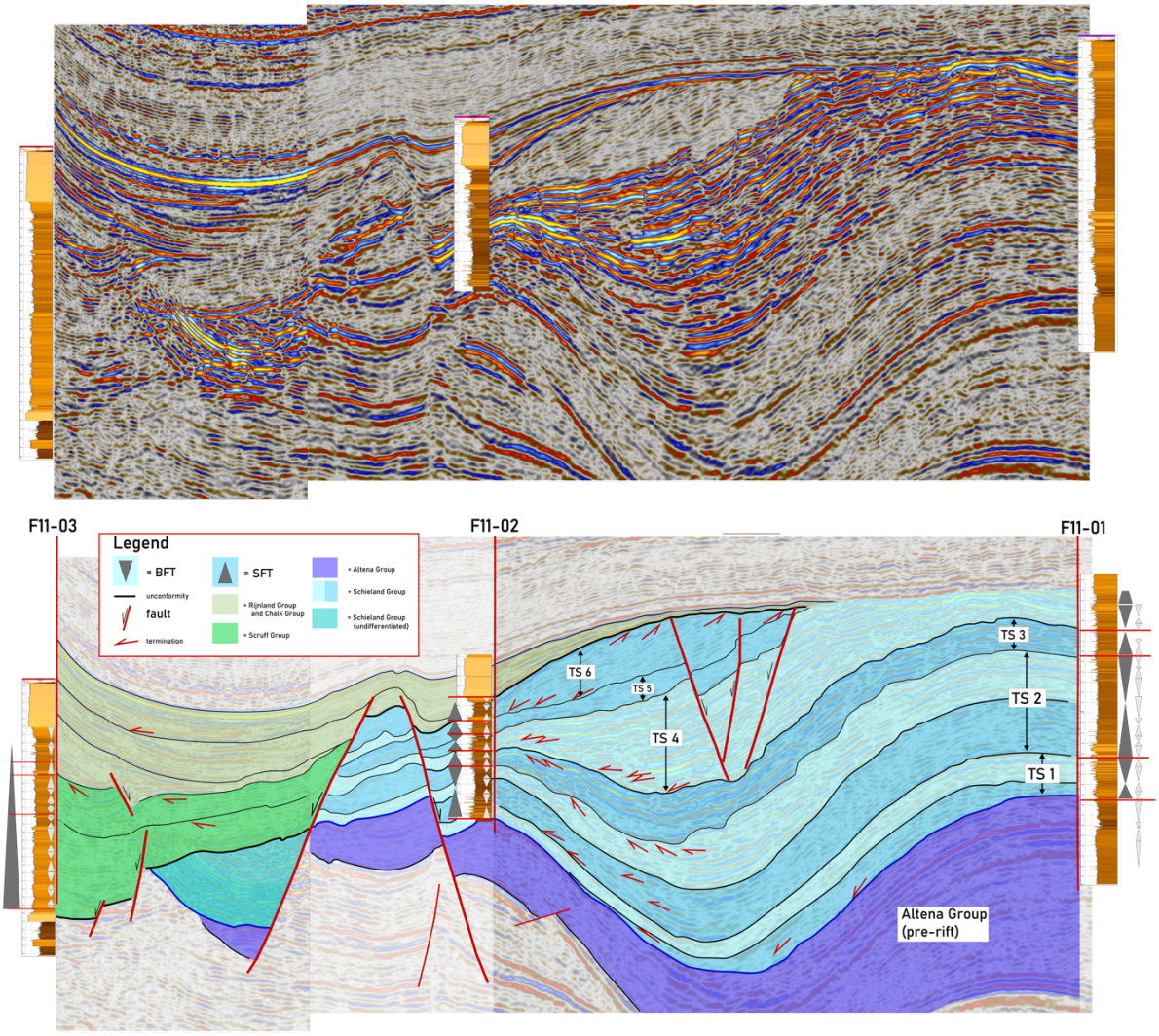

Figure 21. High resolution interpretation of the Upper Jurassic to Lower Cretaceous of section B. This sequence can be subdivided into tectonic successions that have characteristic signatures in well logs and in seismics. For this subdivision, the well log classification scheme in figure 15 and the seismic facies classification scheme in figure 19 are used.

restricted to the center of the basin. This sourceward migrating facies tract onlaps strongly over the underlying Lower Jurassic deposits and can be correlated with facies observed in well F11-01. The subsequent basinward migrating facies tract is correlated with both F11-01 and F11-02, and its distinct high-amplitude seismic facies can be used for predicting lithofacies between wells. The overlying tectonic succession (TS 2) is relatively thick and shows all of the distinctive characteristics that were described for a SFT/BFT alternation. The upper boundary

of this succession is characterized by pronounced angular erosion. This erosion demonstrates to uplift during differential subsidence that occurred during deepening and accommodation space creation for the subsequent tectonic succession. Tectonic successions 2 coincides largely with the estuarine sediment-starved Middle Graben Formation, representing a relatively deep depositional environment. It is overlain by tectonic succession 3 which consists of one single sourceward migrating facies tract, possibly related to strong post-dating erosion. Near the western margin, this tectonic succession also shows strong angular truncation and given the pronounced difference in angle of strata with the overlying sequence, it is very likely that during a phase of strong margin uplift, a significant part of tectonic succession 3 was removed, at least along the western margin. Tectonic succession 3 is overlain by tectonic succession 4 that displays strong thickness variation from basin center to basin margin. In terms of seismic facies, tectonic succession 4 is composed of basinward migrating facies and lacks a clear sourceward migrating facies tract. Overlying tectonic succession 4, two more tectonic successions are observed consisting solely of sourceward migrating facies, with characteristic onlapping reflectors and transparent seismic facies. TS 5 has low amplitude discontinuous intermediate frequency reflectors, whereas TS 6 has similar but slightly more continuous reflectors. The transition from TS 4 to TS 5 is characterized by a sharp change in appearance of seismic reflectors, which can be traced throughout the entire 3D seismic data set.

Section A contains 8 tectonic successions and section contains 6 tectonic successions, in varying degree of completeness that were deposited between the Middle Callovian to the late Early Kimmeridgian. Their typical duration is, around 2 Ma which is significantly longer than the typical duration of a 3rd order sea-level fluctuation in the Jurassic (Haq, 2018). Comparing both sections, there is great similarity in the development of the first two tectonic successions in the basin. These first two tectonic successions coincide largely with the Lower Graben Formation and Middle Graben Formation and are equally developed in both sections. The subsequent sequence of continental and marine siliciclastics of the Puzzle Hole Formation and Kimmeridge Clay Formation shows more pronounced differences between section A and B, in terms of tectonic successions. The tectonic successions in this interval in section B are fragmented. As described, sequences are in some cases composed almost entirely of SFTs or BFTs at the seismic and well-log resolution, which is common in fault-induced rift settings and is controlled by the balance between the rate of creation of accommodation space and sediment supply (Martins-Neto and Catuneanu, 2010; Matenco and Haq, 2020). An initial rapid subsidence or a high sediment supply may create sequences composed entirely of BFTs, such as observed for TS4, while low sediment supply or post-dating erosion may create sequences composed entirely of SFTs, such as observed for TS 5-6.

8. Discussion

8.1 Seismic reconstructions in a regional context

The interpreted sections and their structural reconstruction fit well with existing ideas on general structural style and sedimentation in the Dutch Central Graben. Our observations are in agreement with the general assumption that the thick salt provides an effective decoupling layer for the deformation observed in the over- and under- burden during the Triassic – Early Cretaceous extension (Veen et al., 2012). Deposits of the Callovian to Oxfordian Schieland Group are exceptionally thick and confined to sub-salt fault-bounded basin margins. There is an obvious interplay between the periods of increased fault activity and accelerated salt re-distribution in response to tectonic-induced vertical motions in the underburden and changes in differential loading of the overburden. Despite the difficulty of sub-salt seismic imagery, careful observation indicates clear offset of reflectors below the Zechstein salt, as derived from our interpreted reconstructions (figure 9 to 14). These observations are in line with existing models of thick skinned faulting in the Dutch offshore area (Veen et al., 2012) and earlier structural reconstructions (Winden et al., 2018). Sub-salt faulting occurred due to Jurassic reactivation of earlier (likely Permo-Carboniferous) faults. Where the salt is sufficiently thick, it decouples deformation and prevents faults below the salt to propagate upwards through the salt layer. The brittle deformation of older Permian strata is essentially transferred to a different style of deformation above the salt, the transfer being accommodated by salt re-distribution and the formation of pronounced diapirs at the location of large offset normal faults affecting its underburden (fault F3 and F2 in figure 7 and F1 and F2 in figure 8). Therefore, fault reactivation below the salt controls the location of the basin margin, and salt withdrawal from the basin center is responsible for the observed creation of accommodation space.

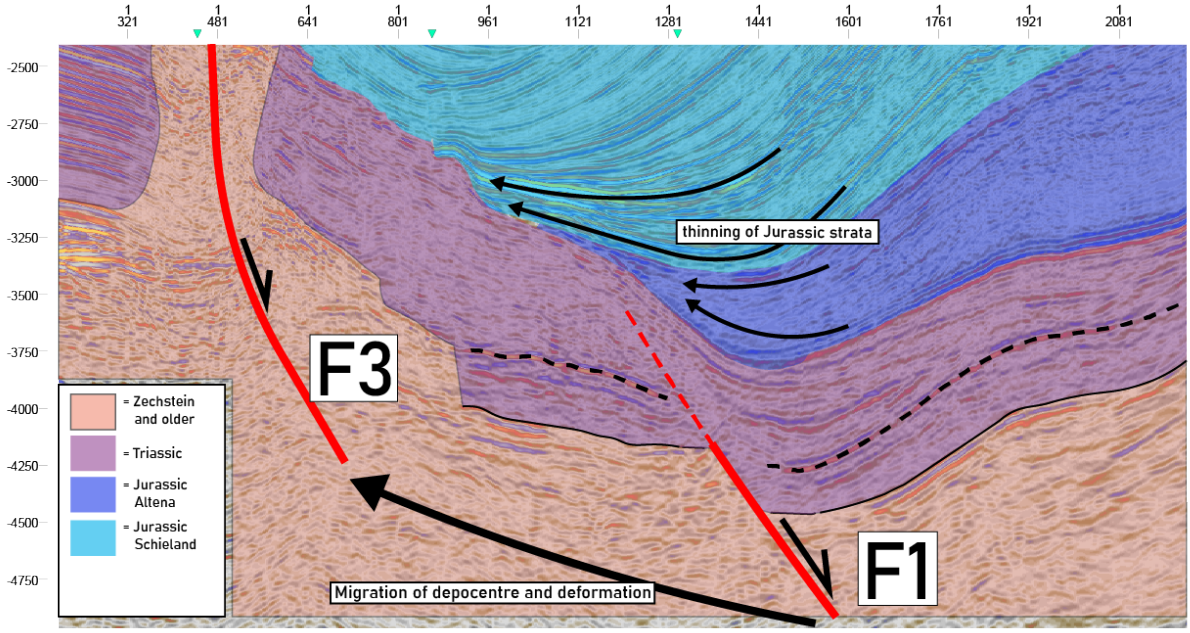

Figure 21. Two main faults in the western part of Section A. Fault F3 marks the margin of the Dutch Central Graben. F1 is a reactivation of an older sub-salt fault. Deformation does not propagate above the salt during the deposition of Jurassic syn-rift sediments. This is different for fault F1. F1 offsets both Zechstein salt as well as Triassic strata. Probably, salt was thin enough around this area to propagate upwards into the post-salt layers. The thinning of the Altena group indicates that this sedimentary unit was syn-depositional to structure F1 whereas younger Jurassic sequences were syn-depositional to F3.

An exception to this clear decoupling of deformation style below and above the salt is the normal fault F1 (figure 7), which offsets both Zechstein salt as well as the Triassic strata. A close-up analysis (figure 21) shows the contrast with another major sub-salt normal fault (F3).

It is likely that salt was locally thin enough at the time of fault F1 formation (due to earlier Triassic salt mobilization) to overcome its rheological decoupling of the ductile layer and propagate upwards. Fault F1 only offsets Triassic strata, but does not affect the overlying Early Jurassic sediments. This behavior may be the result of a more reduced tectonic activity during the Lower Jurassic, or more likely due to a thicker salt layer at the time of its formation (possibly accentuated by the presence of Triassic evaporites), which increases the degree of rheological decoupling. During the Late Jurassic, deformation has probably shifted from fault F1 westwards, where fault F3 accommodated deformation, albeit relatively minor (figure 21).

Another type of salt deformation observed to be accelerated by tectonic episodes is the long-wavelength deformation during the Jurassic – Early Cretaceous expressed by turtle anticlines. The coeval basin infill shows a clear shift in deposition towards the west (figure 7 and 10), which leads to deposition focused along the basin margin, together with uplift and erosion of the former basin center. Our analysis (section B, figure 20) constrains the timing of this change in deformation style to Kimmeridgian. This observation leads to the conclusion that, besides Late Cretaceous or Cenozoic structural inversion, significant uplift and erosion already occurred during the Late Jurassic and was unrelated to compressional far-field tectonic stresses. Instead, it was caused by significant differential salt movements. It is rather clear that the trigger is the depletion of salt in the basin center (salt weld formation) forcing the source of salt flowing towards the diapir to shift towards the margin of the basin (Trusheim, 1960; Vendeville, 2002). The amount of subsidence created to accommodate deposition in these peripheral basins is rather smaller in comparison to the very thick underlying syn-rift sequences. Typically, no significant external tectonic trigger is needed to accommodate the formation of this marginal basin (Peel, 2014).

8.2 Combined seismic and well analysis of tectonic successions

8.2.1 Sub-salt faulting and its relation to syn-kinematic deposition

Our combined high-resolution study of seismics and well logs provide a clear picture of the depositional evolution of the basin. Our derived timing of the onset of Late Jurassic syn-rift sedimentation is in general agreement with the lower resolution previously published interpretations on rift development in the Dutch offshore. The onset of syn-rift sedimentation of the Schieland Group is demonstrated as (Early) Callovian in our combined well and seismic analysis, which agrees with the southward rift propagation (Pharaoh et al., 2010), where onset of syn-rift sedimentation occurs later in the Dutch offshore sector than in the Danish and UK offshore sector (northern extension of the Dutch Central Graben).

At higher resolution, the results of seismic and well log analysis presented in this study point towards a main control of sub-salt faulting and associated salt withdrawal on the alternations of basinward and sourceward migrating facies tracts within the Schieland Group. Firstly, the typical duration of sedimentary cyclicity and associated tectonic successions does not correlate closely with sea-level fluctuations on both 2nd and 3rd order scale (figure 16 & 17). Therefore, a general eustatic driver on the observed sedimentation can be ruled out. The exception is the large global sea-level rise that occurred during the Callovian-Oxfordian (Haq, 2018), which is observed in our study to be coeval with sourceward migrating facies tracts in both sections. This global sea-level rise follows the late Callovian cooling, that is evident from perturbations in isotope records in numerous European basins (Tremolada et al., 2006). The eustatic rise could be the result of the gradual warming that followed this Late Callovian cool period. Possibly, a eustatic control during deposition of the lower part of the Middle Graben Formation has amplified the transgression during the subsidence induced extensional tectonics. Marine palynomorphs that characterize the Callovian Middle Graben Formation claystones indicate

periodic marine influxes that can be attributed to periodic changes from a marginal restricted embayment to a setting with enhanced connection to the marine realm. Secondly, one other observation that demonstrates the main tectonic control is the expression of unconformities bounding basinward migrating and sourceward migrating facies tracts. These unconformities show enhanced expression near the basin margins in response to salt kinematics driven by sub-salt basement faulting. For example, the previously described clear thinning of sourceward migrating seismic facies towards the basin margins illustrates the vertical motion occurring during deposition, meaning relative uplift of the margin and subsidence of the basin center, influenced by structurally induced salt re-distribution and associated creation of accommodation space. Focused deposition in locally evolving depocenters created by salt redistribution further enhanced the potential for salt (re-)distribution.

Despite its clear role in creating accommodation space, it is likely that salt redistribution acted as an enhancer of accommodation space creation and not as an initiator. Salt redistribution is often the result (and thereby an amplifier) of initial tectonic stresses culminating in fault movement, followed by salt redistribution (Jackson and Vendeville, 1994). A classic approach is the idea that diapirism is spontaneously initiated by miniscule irregularities in the interface between salt and the overburden, which gets amplified over time (Trusheim, 1960). However, further work on rock mechanics, specifically on the relative strengths of salt and the overburden, suggests that regional extension localizes, initiates and promotes diapirism of salt and shales. This strengthens the idea that syn-rift sequences (in the Dutch Central Graben) are in the end controlled by fault-related extensional phases, at least in their initial phase of extension initiation. The presence of older Permo-Carboniferous faults below the salt has probably resulted in in the preference of these tectonic stresses to induce reactivation of older sub-salt faults.

8.2.2 Depositional model and lithofacies prediction

We have built a coupled tectonic and salt redistribution depositional model for the Upper Jurassic sedimentary succession of the Dutch Central Graben (figure 22). This model links the observed seismic facies to distinct phases in the development of the basin, where accommodation space is created by fault movement and closely associated salt withdrawal. This model enables a first-order lateral lithofacies prediction. The evolution of the depositional model is illustrated by using a fragment of seismic section A (figure 22). Essentially, the basinward migrating and sourceward migrating facies tracts that make up the tectonic successions represent two dominant phases in the evolution of each individual (sub-)basin. During phases of fault movement and high differential subsidence (enhanced by accelerated salt withdrawal), accommodation space is created and outpaces the rate of sediment supply, resulting in a sourceward migrating facies tract. Characteristic onlap over the margins represents gradual retreat of the system. In some places this might even lead to truncation where local uplift during differential subsidence is strong, best observed in the lower part of the Late Jurassic succession of Section B (figure 21). Sourceward migrating facies tracts are typically composed of predominantly shales and to a lesser extent silts. In the lower parts coarser facies may be observed that gradually retreat during sourceward migration. Such coarser facies are evidenced by reflectors that typically have stronger seismic amplitude closer to the margin (best observed in section A) attesting to lithological contrasts between shales, silts and sands. In addition, flooding of the basin during continued subsidence might locally form laterally extensive coal layers of which the best example can be observed in the Middle Graben Formation or tectonic succession 2 in figure 21. During phases of fault quiescence and low differential subsidence, sediment supply takes over and basinward migrating facies tracts are recorded. Aggradation of strata is observed along the margins, and locally, where seismics are

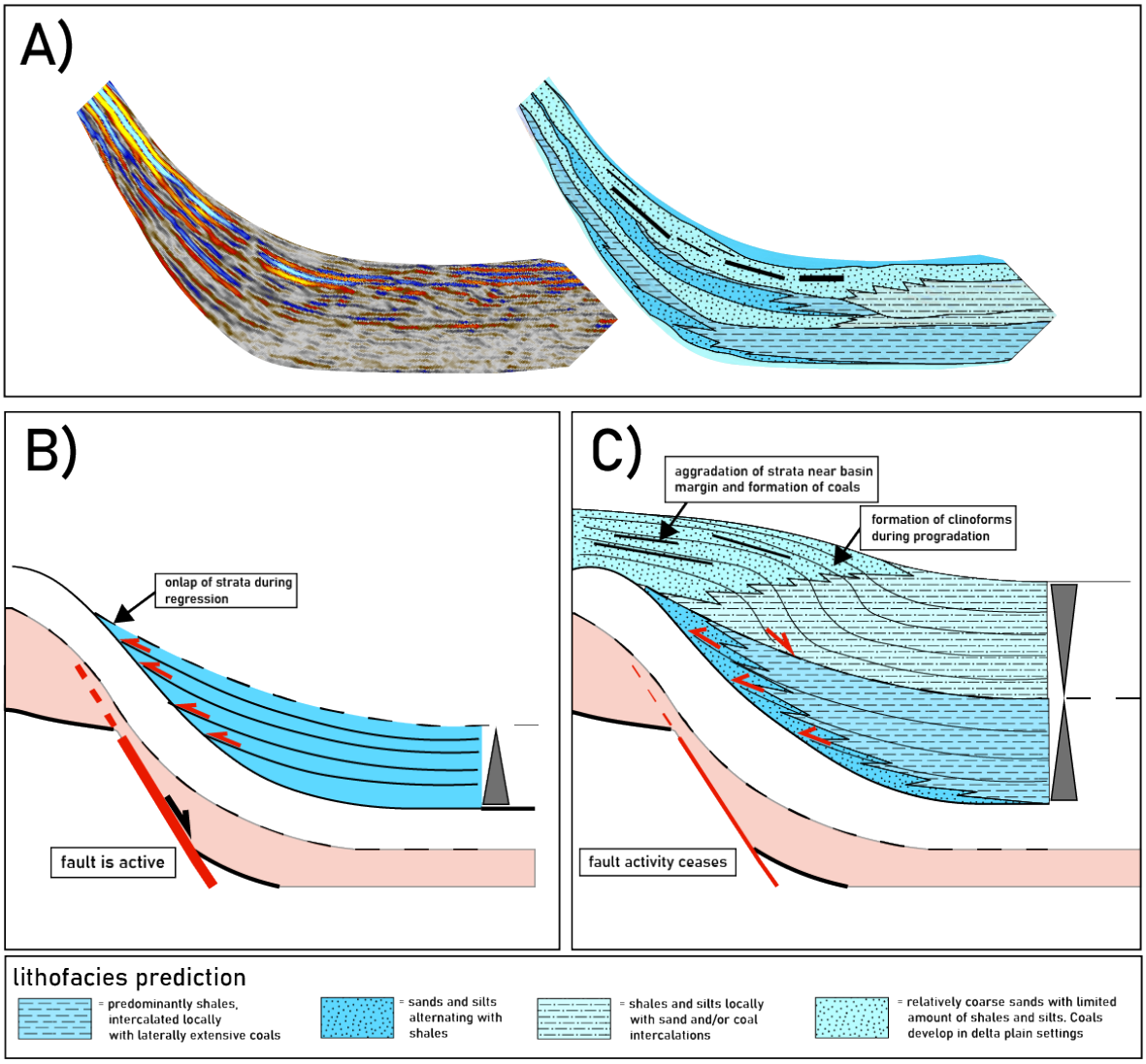

Figure 22. A coupled tectonic and salt redistribution depositional model for the Upper Jurassic deposition in the Dutch Central graben, including a general lithofacies prediction based on well log data and lateral continuation of seismic facies. A shows an uninterpreted and interpreted fragment of seismic section A, which illustrates the alternation between sourceward migrating and basinward migrating facies tracts. Their characteristic features are described in the seismic facies table in figure 19. B & C illustrate the two main phases of a tectonic succession based on the seismics in A. B shows a phase of strong sub-salt fault movement, differential subsidence and associated uplift in the diapirs, resulting in a sourceward migrating facies tract. C shows the subsequent cessation of tectonic movement and deposition of a basinward migrating facies.

of high enough resolution relative to the sedimentation rate, clinoformal geometries and downlaps can be observed (figure 22). BFT's are relatively sand-rich and form fluvial/deltaic channel or tidal flat geometries that intercalate with shales. Laterally these may grade into finer grained deposits composed of shales and silts, basinwards. Especially in the Oxfordian to Kimmeridgian Puzzle Hole Formation, relatively discontinuous coal layers become frequent. These coals have likely accumulated in delta plain settings in the more proximal areas, behind clinoformal geometries as observed in figure 22A. Intervals with these coals have very high amplitude reflectors and are expressed most strongly along the margins of the basin.

8.2.3 Local variation in the deposition of tectonic successions

The observed differences between section A and section B are caused by local factors driving the overall regional variation in the development of tectonic successions. Section A shows a much more gradual change (from predominantly basinward migrating facies towards

predominantly sourceward migrating facies) than observed in the similar interval in section B. Also, section A is composed of alternations of overall complete tectonic successions. In contrast, TS4 in section B is composed of a single BFT, whereas TS 5 and 6 consist only of SFT's.

Several important factors have had a potential role in creating this difference, of which some might have acted during deposition. TS 4 in section B might have been deposited during a phase when initial rapid subsidence (evidenced by the angular truncation of underlying TS3) was followed by high sediment supply and predominantly basinward migrating facies. Between TS4 and TS5 a prolonged period of non-deposition occurred after which TS5 and TS6 were deposited consisting of single SFT's during phases of relatively low sediment supply. We hypothesize that fault F1 in section A created more continuous and regular alternation of tectonic activity and tectonic quiescence whereas the absence of such a strong controlling fault in section B caused a more incomplete and fragmented succession. The sedimentary sequence in Section B was likely more prone to irregular salt withdrawal and long wavelength deformation of salt, possibly expressed in the anti- and syn-forms that are stronger in section B than in section A (comparing figure 20 and 21). Exact quantification of the complex role of salt movement is beyond the scope of our work. But evidently, local forcing factors created significant difference in development of tectonic succession within a relatively small distance.

8.2.4 Implications for current tectonostratigraphic framework

Our results shed light on the existing broad subdivision of Late Jurassic to Early Cretaceous sequences into the previously described Tectonic Megasequences (e.g., Bouroullec et al., 2018). The tectonic successions approach defines depositional sequences on a significantly higher resolution than the current stratigraphic framework. Within TMS-1 ((Verreussel et al., 2018) we define at least 6 to 8 distinguishable tectonic successions. In addition, the style and periodicity of sedimentary cyclicity differs between the initial Schieland Group continental facies and the overlying shallow marine to open marine facies of the Scruff Group (Lies member). This change in the apparent sedimentary cyclicity coincides with a depositional shift

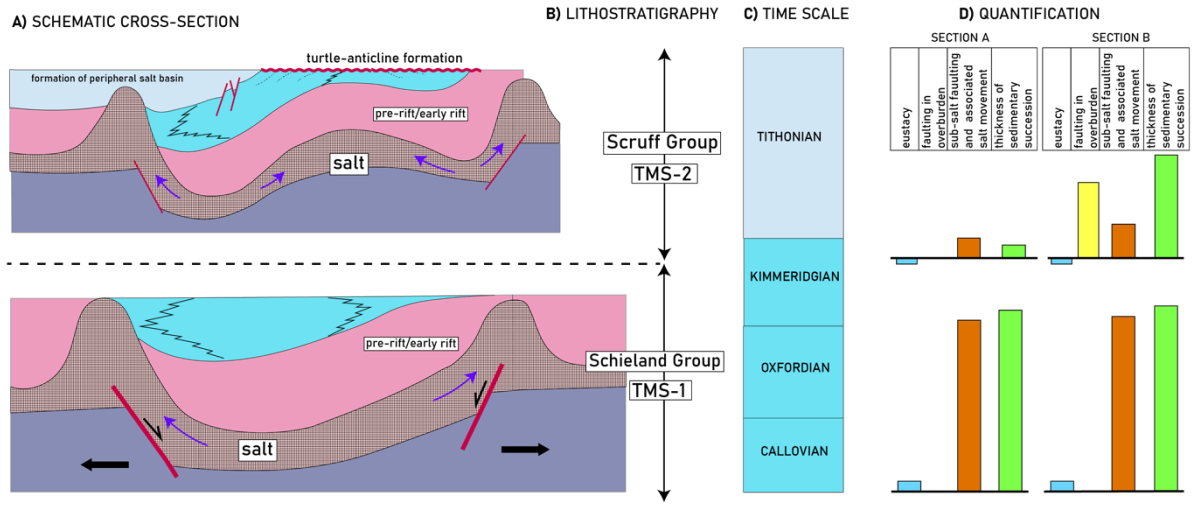

Figure 23. Hypothetical depositional model for the studied area in two phases, illustrated in a representative schematic cross section (A). D shows a quantification of the different controlling factors (thickness of successions, magnitude of vertical motion along a fault or salt structure, and magnitude of sea-level change during a specific period). This enables a distinction between the two depositional phases, based on quantification. The first phase (Callovian – Kimmeridgian) is characterized by the deposition of tectonic successions, controlled by strong sub-salt faulting. During the second phase (Tithonian) a relative decrease of sub-salt faulting occurs, connection to the marine realm is established and a change in salt migration results in turtle anticline formation, axial erosion and deposition along the basin margin. Sedimentary cyclicity is controlled by 3rd order sea-level fluctuation, observed in our well analysis of F11-03 (figure 18).

from basin center towards basin margin, evident from the results of our structural reconstruction. The combination of these observations suggests a change in sedimentation that is closely linked to the structural style. Thickness estimations of sedimentary sequences in both sections, combined with estimations of vertical motion along structures and known magnitudes of sea-level change enable a comparison of the relative contribution of different factors (figure 23) in deposition of the Schieland (primary salt basin) and Scruff Groups (peripheral salt basin). The combined influence of these factors results in the observed thickness of a sedimentary succession. This quantification (figure 23D) suggests that the role of sub-salt fault movement and associated salt redistribution must have been significantly higher during Schieland Group deposition than during Scruff Group deposition.

With respect to this observation, we hypothesize that the Schieland Group siliciclastics are strongly controlled by alternating phases of tectonic activity and tectonic quiescence. On the contrary, the peripheral salt basin phase (Scruff Group) was accommodated by significantly reduced sub-salt tectonic activity (relative to Schieland Group deposition), salt weld formation

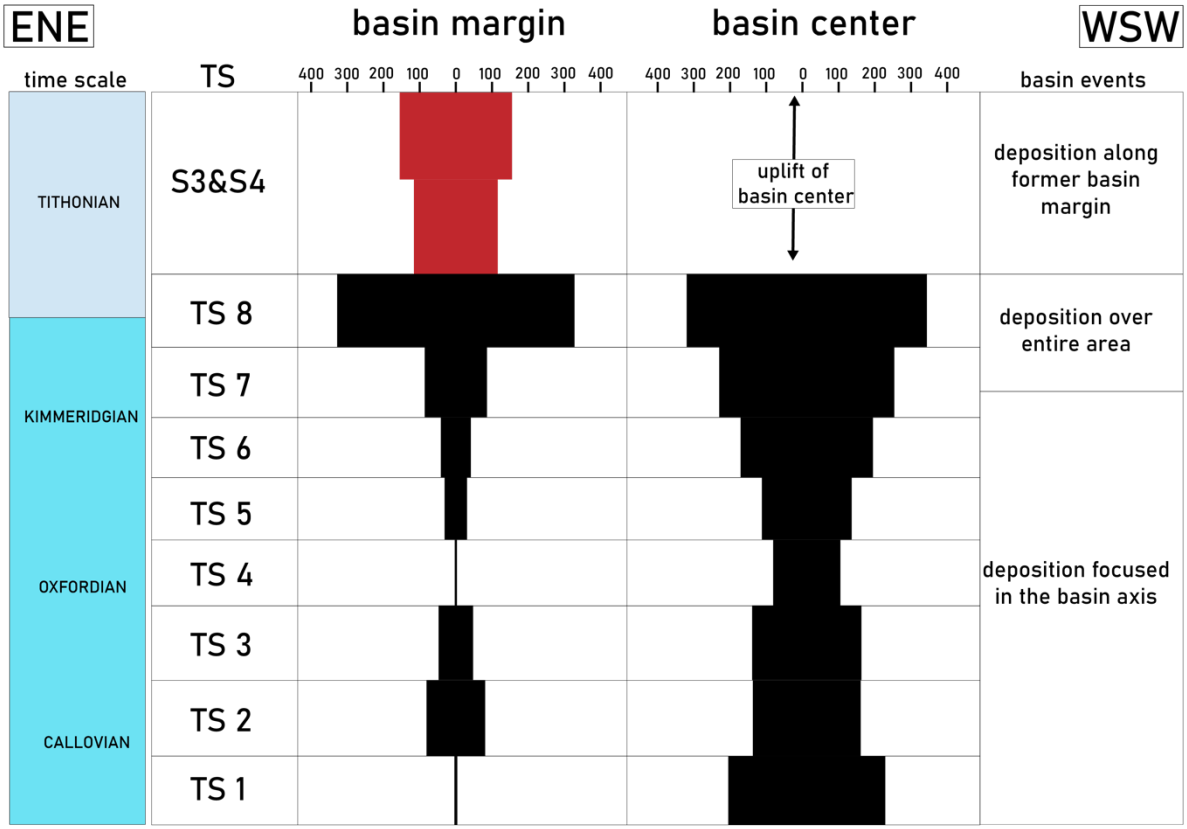

Figure 24. Quantification of subsidence through space and over time in section A, using the novel tectonic succession framework. Black squares depict the thickness of the successions and thereby illustrate the degree of subsidence during deposition, both along the basin margin as well as in the basin center. Note that the different TS's are assumed to be roughly equal in duration (typically between 2 and 3 Ma) and that the time scale is a rough estimation based on biostratigraphic constrains from the nearby section B. Specific biostratigraphic dating for section A is not available.

in the basin center and salt migration with a salt source located along the basin margins, and locally presence of active faults in the overburden creating accommodation space (like in section B). The 0.8 Ma sedimentary cyclicity observed in F11-03 for the Scruff Group indicates the disappearance of clear 2-3 Ma tectonic pulses as observed for the Schieland Group. Instead, cyclicity here strongly correlates to 3rd order sea-level fluctuations (figure 18), possibly enhanced by restored connection to sea-level.

The detection of tectonic successions enables further quantification of the tectonic pulses that are represented by tectonic successions. Such quantification is based on the thickness of the subsequent successions and their variation through space and over time (figure 24). This illustrates that the initial phase of tectonic subsidence is focused on the basin center. Subsidence is relatively strong during deposition of TS1 followed by a relative weakening of subsidence (TS2-TS4) which is subsequently followed by the strongest phase of subsidence in the basin axis (TS6-TS8) which is coeval with strong subsidence along the margin. Finally, sequences S3 and S4 are deposited along the margin, coeval with uplift of the basin center.

8.3 Models for the interplay between tectonics and sedimentation in salt influenced basins

Our results contribute to an improved understanding of the interplay between sedimentation, tectonics and salt mobilization, together with new insights on the associated facies distribution in extensional salt basins.

The distribution of facies in the tectonic-driven phase of the Dutch Central Graben differs from the typical facies' distribution in fault-bounded asymmetric half-grabens or sub-basins, in space and over time. We observe that lateral changes in facies are significantly less expressed or more subtle in salt basins. This is best illustrated by the great similarity in well log facies and lithology between well F11-01 (located in the basin center) and well F11-02 (located along the basin margin). The only significant difference between wells is the thickness of the entire Late Jurassic succession, but changes in the lithological trends are subtle. In addition, our lithofacies prediction, based on seismic facies analysis indicates that lateral variation in

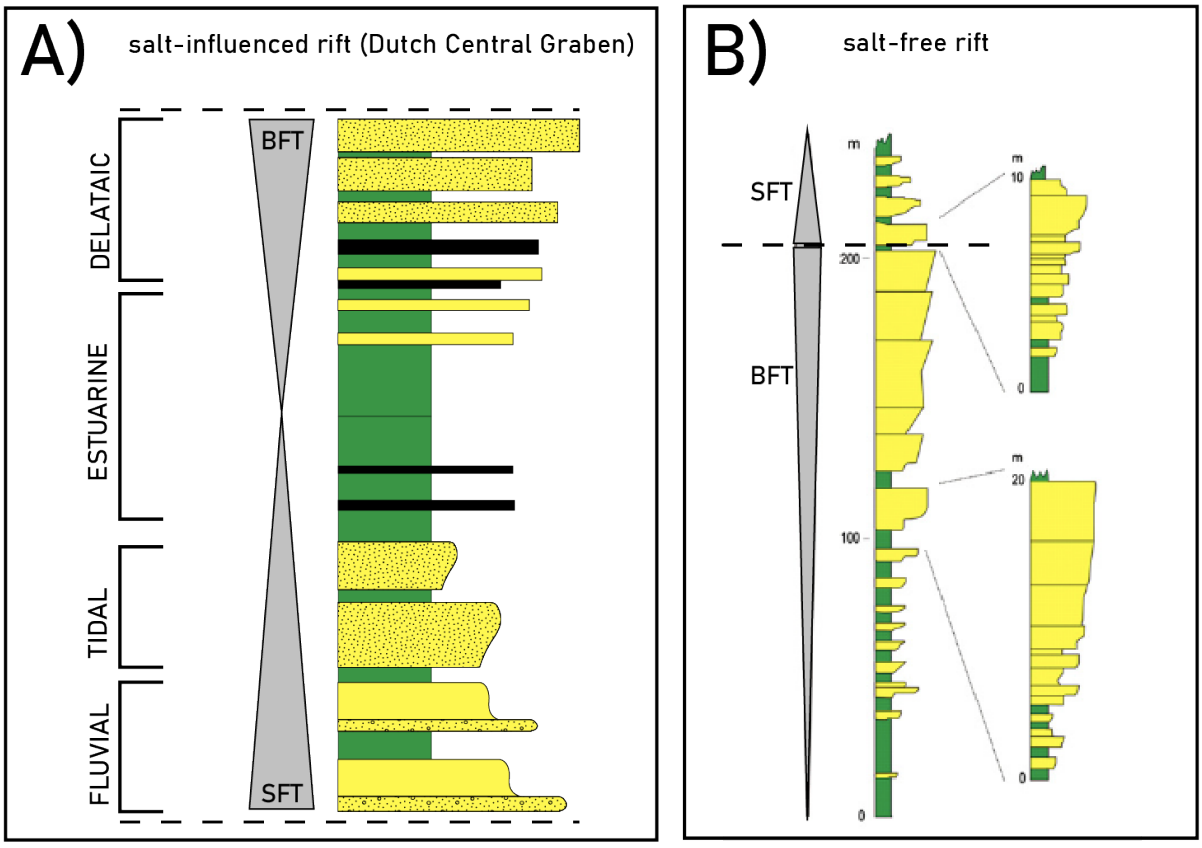

Figure 25. Conceptual model of a rift (sub-)basin tectonic succession in a salt-influenced and a salt-free system. A) a salt-influenced syn-rift tectonic succession comprises equally well-developed basinward and sourceward migrating facies tracts. B) A typical syn-rift succession in an alluvial-lacustrine fault-bounded basin. The succession is dominated by the basinward migrating facies tract. Due to rapid deepening during fault activity, a sourceward migrating facies tract is thin or absent (modified from Martins-Neto and Catuneanu, 2010).

lithology throughout sections are minimal (figure 22). Data from the northern part of the Central Graben system, in the Norwegian sector, shows similar style of facies distribution. Stratal thickness changes are also observed across salt structures, but facies variability across these structures is likely limited (Mannie et al., 2016). This is different from the abrupt lateral facies changes that typically occur in fault-bounded half-grabens (Prosser, 1993), which are not evident in our study area either laterally or vertically.

Another illustrative feature of facies distribution in salt basins is their variation throughout vertical sections. The facies observed in F11-01 and F11-02 alternate between estuarine/lagoonal to more deltaic and continental/fluvial facies. These changes are commonly gradual indicating that sudden deepening due to fault activity does not occur. Sourceward migrating facies tracts are equally thick as basinward migrating facies tracts, in contrast to continental rift settings where rift sequences may commonly exist of a single or very thick basinward migrating facies tract and a significantly thinner sourceward migrating facies tract (Martins-Neto and Catuneanu, 2010; Matenco and Haq, 2020). Two conceptual sedimentary logs that demonstrate this difference are depicted in figure 25.

Our observations in terms of facies distribution in the salt-influenced Dutch Central Graben are in agreement with earlier studies on syn-depositional topography and its influence on sedimentation. Sediment pathways in the Dutch Central Graben do not follow the typical models implying axial sediment distribution trends during early phases of rifting (Leeder and Gawthorpe, 1987; Prosser, 1993). Rather, seismic attribute maps of the Dutch Central Graben indicate that sediment pathways were oriented mostly perpendicular to the structural grain, in fluvio-deltaic sedimentary systems (Bouroullec et al., 2018). This observation agrees with the notion that basin physiography in salt basins is characterized by relatively low gradients and gentle topography, rather than sharp changes in gradient created by strong fault propagation (Banham and Mountney, 2013). The absence of significant lateral facies changes is similar to other areas where extensional deformation is accompanied by halokinesis. Previous studies have shown that observations from the Late Jurassic stratigraphy of the Central Lusitanian Basin (west Iberia) indicate a clear difference between diapir-bounded and fault-bounded sub-basins (Alves et al., 2003). These studies have shown that a distinct low-gradient basin physiography, which develops in salt-bounded sub-basins, results in the deposition of axial to hanging-wall-derived deltaic/shallow-marine deposits with minor turbiditic content, which is in sharp contrast with the presence of more gravity-driven depositional system with high facies variability and abrupt facies changes in fault-bounded basins.

8.4 Applications subsurface resources

Our results are certainly important for societally relevant applications of the subsurface such as the current hydrocarbon exploration or for sustainable use of subsurface reservoirs in the future (Doornenbal et al., 2019).

The Late Jurassic sequences of the Dutch Central Graben (Lower Graben Formation, Middle Graben Formation and Puzzle Hole Formation) have potential reservoir properties and may form part of a successful play (Abbink et al., 2006). Within this play, the Lower Jurassic Posidonia Shale Formation or to a lesser extent the coal seems in the Middle Graben Formation may have acted as source rock intervals. Sandy channel bodies within the Graben Formations are potential reservoirs that accumulated hydrocarbons originating from these source rock intervals. The enclosing shales within the Graben Formation may act as stratigraphic traps, depending on their quality and sealing capacity, possibly complicated by small breaches due to soil formation (Abbink et al., 2006). The very obvious turtle structures (figure 8) may have

formed broader structural trap configurations. Such a structural configuration has proven successful in the F-03 field, for example (Bouroullec et al., 2018). The high-resolution analysis presented in this study potentially contributes to further understanding of Late Jurassic play types in the Dutch Central Graben. Most importantly, it provides a powerful predictive tool that strengthens the ability to locate basinward and sourceward migrating facies tracts and their distinctive lithological properties. It also contributes to a better understanding of their structural configurations and controlling mechanisms.

9. Conclusion

We present a combined seismic and well analysis of the Jurassic to Early Cretaceous basin infill of the Dutch Central Graben. Our first-order seismic interpretation differentiates three distinct phases of basin development. Starting from the Callovian, a thick syn-rift sequence is deposited which is focused on the center of the Dutch Central Graben and thins towards bounding salt bodies that overlie sub-salt faults. During the Kimmeridgian, deposition shifts to the margins of the basin due to depletion of salt in the basin center and onset of salt migration sourced from the margins. Late Kimmeridgian and Tithonian sedimentary wedges thin towards and onlap over the basin center. This depositional shift is coeval with turtle anticline formation and erosion of the Late Jurassic basin axis. The third phase is a Cretaceous inversion phase that is expressed in angular truncation over large parts of the two studied section, caused by upwarp of a significant part of the area related to compressional forces.

Our first-order interpretation is complemented with a quantitative high resolution seismic and well log facies model that enables detection of sourceward migrating and basinward migrating facies tracts within the siliciclastic Jurassic Schieland Group, forming tectonic successions. These successions have formed in response to differential subsidence of the salt-bounded margins, controlled by sub-salt fault movement. Sourceward migrating facies typically onlap over the basin margin and are characterized by low amplitude reflectors, especially in the distal parts of the basin. They show significant lateral thickness variation and correlate in wells with fining upward sequences. Basinward migrating facies have higher amplitude reflectors and typically show aggradation of strata near the margin. Locally, they display clinoformal geometries that downlap on underlying strata, indicating progradation during periods when sediment supply outpaces accommodation space creation. They correlate with coarsening upward trends in wells. Tectonic successions, comprised of BFT's and SFT's , have a typical duration of 2-3 Ma (based on biostratigraphic constraints in well F11-01 and F11-02) and do not correlate to sea-level fluctuation on 2nd or 3rd order scale (Haq, 2018). We hypothesize that their alternation is controlled by periods of tectonic activity and tectonic quiescence controlled by reactivation of sub-salt Permo-Carboniferous faults in combination with closely associated re-distribution of Zechstein salt.

By detecting tectonic successions, we contribute to better understanding of the area in several ways. We build upon and differentiate the current stratigraphic framework (Bouroullec et al., 2018), on a regional scale. We observe 6 to 8 tectonic successions within the Late Jurassic Schieland Group, in both section A and section B. Furthermore, we observe differences in the development of these tectonic successions across the basin, between the northern part (section A) and the southern part (section B). Section A shows a more complete and continuous alternation of SFT's and BFT's whereas Section B shows a more fragmented succession of tectonic successions characterized by incomplete successions and more abrupt changes seismic facies. We propose several potential contributing factors that might have caused this difference. Possibly, there was stronger and more continuous subsidence in the northern part of the area, possibly related to the presence of fault F1 in section A (figure 7). In addition, the southern

part might have been influenced by periods of higher relative sediment supply or by significant periods of erosion and removal of parts of tectonic successions.

Furthermore, we hypothesize that controlling mechanisms differed between the Schieland Group (basin axis phase) and the Scruff Group (peripheral basin phase). Quantification of eustasy, overburden faulting, and thickness of sedimentary successions for these groups indicates that tectonic subsidence created by sub-salt faults and associated salt (re-)distribution was significantly stronger during deposition of the Schieland Group than during deposition of the Scruff Group. The weakened role of strong phases of tectonic subsidence and quiescence related to basement faulting can explain the expression of sedimentary cyclicity of the Scruff Group closely linked to 3rd order sea level fluctuations with a typical periodicity of 0.8 Ma. This is in contrast with the 2-3 Ma periodicity of sedimentary cycles and tectonic successions during deposition of the Schieland Group. Finally, we demonstrate, in confirmation with other studies in different basins, that facies do not change as rapidly across space and over time in salt influenced rift basins as in fault-bounded basins. This is a result of the very gentle syndepositional topography that is created by the salt that decouples faults from the overburden.

10. Acknowledgements

First of all, I would like to thank Liviu Matenco for his generous support during this project. I have benefitted a lot from his constructive suggestions and his rapid and focused responses on my questions. Fadi Nader is thanked for reviewing my results in an earlier stage and reading the final report.

Marten ter Borgh, Kees van Ojik and Daan den Hartog Jager from EBN are thanked for their critical review of some early versions of my work and the opportunity they gave to present my work for other experts on the Dutch offshore. Also, I would like to thank Total for allowing me to use the F11F12_Z3TOTAL2012 Survey in my report. This has enabled optimal graphical quality of the seismic data used in this study.

11. References

Abbink, O.A., Mijnlieff, H.F., Munsterman, D.K., Verreussel, R.M.C.H., 2006. New stratigraphic insights in the 'Late Jurassic' of the Southern Central North Sea Graben and Terschelling Basin (Dutch Offshore) and related exploration potential. Netherlands Journal of Geosciences 85, 221–238. https://doi.org/10.1017/S001677460002148X

Alves, T.M., Manuppella, G., Gawthorpe, R.L., Hunt, D.W., Monteiro, J.H., 2003. The depositional evolution of diapir- and fault-bounded rift basins: examples from the Lusitanian Basin of West Iberia. Sedimentary Geology 162, 273–303. https://doi.org/10.1016/S0037-0738(03)00155-6

Andsbjerg, J., 2003. Sedimentology and sequence stratigraphy of the Bryne and Lulu Formations, Middle Jurassic, northern Danish Central Graben. GEUS Bulletin 1, 301–347. https://doi.org/10.34194/geusb.v1.4676

Banham, S.G., Mountney, N.P., 2013. Evolution of fluvial systems in salt-walled mini-basins: A review and new insights. Sedimentary Geology 296, 142–166. https://doi.org/10.1016/j.sedgeo.2013.08.010

Bouroullec, R., Verreussel, R.M.C.H., Geel, C.R., Bruin, G. de, Zijp, M.H. a. A., Kőrösi, D., Munsterman, D.K., Janssen, N.M.M., Kerstholt-Boegehold, S.J., 2018. Tectonostratigraphy of a rift basin affected by salt tectonics: synrift Middle Jurassic–Lower Cretaceous Dutch Central Graben, Terschelling Basin and neighbouring platforms, Dutch offshore. Geological Society, London, Special Publications 469, 269–303. https://doi.org/10.1144/SP469.22

Catuneanu, O., 2019a. Model-independent sequence stratigraphy. Earth-Science Reviews 188, 312–388. https://doi.org/10.1016/j.earscirev.2018.09.017

Catuneanu, O., 2019b. Scale in sequence stratigraphy. Marine and Petroleum Geology 106, 128–159. https://doi.org/10.1016/j.marpetgeo.2019.04.026

Doornenbal, J.C., Kombrink, H., Bouroullec, R., Dalman, R. a. F., Bruin, G.D., Geel, C.R., Houben, A.J.P., Jaarsma, B., Juez-Larré, J., Kortekaas, M., Mijnlieff, H.F., Nelskamp, S., Pharaoh, T.C., Veen, J.H.T., Borgh, M.T., Ojik, K.V., Verreussel, R.M.C.H., Verweij, J.M., Vis, G.-J., 2019. New insights on subsurface energy resources in the Southern North Sea Basin area. Geological Society, London, Special Publications 494. https://doi.org/10.1144/SP494-2018-178

Geluk, M.C., 2005. Stratigraphy and tectonics of Permo-Triassic basins in the Netherlands and surrounding areas [WWW Document]. URL http://localhost/handle/1874/1699 (accessed 10.8.20).

Haq, B.U., 2018. Jurassic Sea-Level Variations: A Reappraisal. GSAT 4–10. https://doi.org/10.1130/GSATG359A.1

Haq, B.U., 2014. Cretaceous eustasy revisited. Global and Planetary Change 113, 44–58. https://doi.org/10.1016/j.gloplacha.2013.12.007

Haq, B.U., Hardenbol, J., Vail, P.R., 1988. Mesozoic and Cenozoic Chronostratigraphy and Cycles of Sea-Level Change.

Herngreen, G.F.W., Kouwe, W.F.P., Wong, T.E., 2003. The Jurassic of the Netherlands. GEUS Bulletin 1, 217–230. https://doi.org/10.34194/geusb.v1.4652

Jackson, M.P.A., Vendeville, B.C., 1994. Regional extension as a geologic trigger for diapirism. GSA Bulletin 106, 57–73. https://doi.org/10.1130/0016-7606(1994)106<0057:REAAGT>2.3.CO;2

Leeder, M.R., Gawthorpe, R.L., 1987. Sedimentary models for extensional tilt-block/half-graben basins. Geological Society, London, Special Publications 28, 139–152. https://doi.org/10.1144/GSL.SP.1987.028.01.11

Mannie, A.S., Jackson, C.A.-L., Hampson, G.J., Fraser, A.J., 2016. Tectonic controls on the spatial distribution and stratigraphic architecture of a net-transgressive shallow-marine synrift succession in a salt-influenced rift basin: Middle to Upper Jurassic, Norwegian Central North Sea. Journal of the Geological Society 173, 901–915. https://doi.org/10.1144/jgs2016-033

Martins-Neto, M.A., Catuneanu, O., 2010. Rift sequence stratigraphy. Marine and Petroleum Geology 27, 247–253. https://doi.org/10.1016/j.marpetgeo.2009.08.001

Matenco, L.C., Haq, B.U., 2020. Multi-scale depositional successions in tectonic settings. Earth-Science Reviews 200, 102991. https://doi.org/10.1016/j.earscirev.2019.102991

Mitchum, R.M., Vail, P.R., Iii, S.T., 1977. Seismic Stratigraphy and Global Changes of Sea Level: Part 2. The Depositional Sequence as a Basic Unit for Stratigraphic Analysis: Section 2. Application of Seismic Reflection Configuration to Stratigraphic Interpretation 165, 53–62.

Munsterman, D.K., Verreussel, R.M.C.H., Mijnlieff, H.F., Witmans, N., Kerstholt-Boegehold, S., Abbink, O.A., 2012. Revision and update of the Callovian-Ryazanian Stratigraphic Nomenclature in the northern Dutch offshore, i.e. Central Graben Subgroup and Scruff Group.

Neal, J.E., Abreu, V., Bohacs, K.M., Feldman, H.R., Pederson, K.H., 2016. Accommodation succession (δA/δS) sequence stratigraphy: observational method, utility and insights into sequence boundary formation. Journal of the Geological Society 173, 803–816. https://doi.org/10.1144/jgs2015-165

Ogg, J.G., Ogg, G.M., Gradstein, F.M., 2016. A Concise Geologic Time Scale: 2016. Elsevier.

Peel, F.J., 2014. How do salt withdrawal minibasins form? Insights from forward modelling, and implications for hydrocarbon migration. Tectonophysics 630, 222–235. https://doi.org/10.1016/j.tecto.2014.05.027

Pharaoh, T.C., Dusar, M., Geluk, M., Kockel, F., Krawczyk, C.M., Krzywiec, P., Scheck-Wenderoth, M., Thybo, H., Vejbaek, O., Van Wees, J.-D., 2010. Chapter 3: Tectonic Evolution, Petroleum Geological Atlas of the Southern Permian Basin Area. EAGE.

Prosser, S., 1993. Rift-related linked depositional systems and their seismic expression. Geological Society, London, Special Publications 71, 35–66. https://doi.org/10.1144/GSL.SP.1993.071.01.03

Remmelts, G., 1996. Salt tectonics in the southern North Sea, the Netherlands, in: Rondeel, H.E., Batjes, D.A.J., Nieuwenhuijs, W.H. (Eds.), Geology of Gas and Oil under the Netherlands: Selection of Papers Presented at the 1983 Iternational Conference of the American Association of Petroleum Geologists, Held in The Hague. Springer Netherlands, Dordrecht, pp. 143–158. https://doi.org/10.1007/978-94-009-0121-6_13

Remmelts, G., 1995. Fault-Related Salt Tectonics in the Southern North Sea, The Netherlands 261–272.

Trabucho-Alexandre, J., Dirkx, R., Veld, H., Klaver, G., de Boer, P.L., 2012. Toarcian Black Shales In the Dutch Central Graben: Record of Energetic, Variable Depositional Conditions During An Oceanic Anoxic Event. Journal of Sedimentary Research 82, 104–120. https://doi.org/10.2110/jsr.2012.5

Tremolada, F., Erba, E., van de Schootbrugge, B., Mattioli, E., 2006. Calcareous nannofossil changes during the late Callovian–early Oxfordian cooling phase. Marine Micropaleontology 59, 197–209. https://doi.org/10.1016/j.marmicro.2006.02.007

Trusheim, F., 1960. Mechanism of Salt Migration in Northern Germany. AAPG Bulletin 44, 1519–1540. https://doi.org/10.1306/0BDA61CA-16BD-11D7-8645000102C1865D

Underhill, J.R., Partington, M.A., 1993. Jurassic thermal doming and deflation in the North Sea: implications of the sequence stratigraphic evidence. Petroleum Geology of

Northwest Europe: Proceedings of the 4th Conference 337–345. https://doi.org/10.1144/0040337
Van Adrichem Boogaert, H.A., Kouwe, W.P.F., 1993. Stratigraphic nomenclature of the Netherlands, revision and update by RGD and NOGEPA. Med. Rijks geol. Dienst pag. mult.
van Wees, J.-D., Stephenson, R.A., Ziegler, P.A., Bayer, U., McCann, T., Dadlez, R., Gaupp, R., Narkiewicz, M., Bitzer, F., Scheck, M., 2000. On the origin of the Southern Permian Basin, Central Europe. Marine and Petroleum Geology 17, 43–59. https://doi.org/10.1016/S0264-8172(99)00052-5
Van Wijhe, D.H., 1987. Structural evolution of inverted basins in the Dutch offshore. Tectonophysics 137, 171–219. https://doi.org/10.1016/0040-1951(87)90320-9
Veen, J.H. ten, Gessel, S.F. van, Dulk, M. den, 2012. Thin- and thick-skinned salt tectonics in the Netherlands; a quantitative approach. Netherlands Journal of Geosciences 91, 447–464. https://doi.org/10.1017/S0016774600000330
Vendeville, B.C., 2002. A New Interpretation of Trusheim's Classic Model of Salt-Diapir Growth 52, 943–952.
Verreussel, R.M.C.H., Bouroullec, R., Munsterman, D.K., Dybkjær, K., Geel, C.R., Houben, A.J.P., Johannessen, P.N., Kerstholt-Boegehold, S.J., 2018. Stepwise basin evolution of the Middle Jurassic–Early Cretaceous rift phase in the Central Graben area of Denmark, Germany and The Netherlands. Geological Society, London, Special Publications 469, 305–340. https://doi.org/10.1144/SP469.23
Wagoner, J.C.V., Mitchum, R.M., Campion, K.M., Rahmanian, V.D., 1990. Siliciclastic Sequence Stratigraphy in Well Logs, Cores, and Outcrops: Concepts for High-Resolution Correlation of Time and Facies. https://doi.org/10.1306/Mth7510
Winden, M. van, Jager, J. de, Jaarsma, B., Bouroullec, R., 2018. New insights into salt tectonics in the northern Dutch offshore: a framework for hydrocarbon exploration. Geological Society, London, Special Publications 469, 99–117. https://doi.org/10.1144/SP469.9
Wong, T.E., Batjes, D.A.J., Jager, J. de, Koninklijke Nederlandse Akademie van Wetenschappen, 2007. Geology of the Netherlands. Royal Netherlands Academy of Arts and Sciences : Information and orders, Edita-KNAW, Amsterdam, Netherlands.
Ziegler, P.A., 1990. Collision related intra-plate compression deformations in Western and Central Europe. Journal of Geodynamics, Intracontinental Mountainous Terranes 11, 357–388. https://doi.org/10.1016/0264-3707(90)90017-O